Managing for ecological surprises in metapopulations

Supplemental materials: Model details & results

Kyle L. Wilson[a]*, Alex Sawyer[a], Anna Potapova[a], Colin J. Bailey[a], Elissa Sweeney-Bergen[a], Emma E. Hodgson[a], Kara J. Pitman[a], Karl Seitz[a], Lauren Law[a], Luke Warkentin[a], Samantha M. Wilson[a], William I. Atlas[a], Daniella LoScerbo[b], Douglas C. Braun[c], Matthew R. Sloat[d], M. Tim Tinker[e], and Jonathan W. Moore[a,b]

[a]Earth to Ocean Research Group, Simon Fraser University
[b]Resource and Environmental Management, Simon Fraser University
[c]Fisheries and Oceans Canada
[d]Wild Salmon Center
[e]Ecology and Evolutionary Biology, University of California Santa Cruz

16 September 2019

Contents

*Corresponding author - email: kl_wilson@sfu.ca

Metapopulation model

Local & metapopulation dynamics

Our metapopulation is defined by a set of local populations N_p for a species with a one year generation time with time-dynamics that follows birth (i.e., recruitment R), immigration, death, and emigration (BIDE) processes typical to metapopulation theory (Hanski 1998):

$$N_{it+1} = R_{it}\epsilon_{it} + I_{it} - D_{it} - E_{it} \tag{1}$$

where N_{it+1} is the number of adults in patch i at time t, R_{it} is number of recruits, I_{it} is number of recruits immigrating into patch i from any other patch, D_{it} is number of recruits that die due to disturbance regime, E_{it} is the number of recruits emigrating from patch i into any other patch, and ϵ_{it} is stochasticity in recruitment.

Resoure monitoring often occurs at the scale of the metapopulation (Anderson et al. 2015), hence we define metapopulation adults as:

$$MN_t = \sum_{i=1}^{N_p} N_{it} \tag{2}$$

with metapopulation recruits:

$$MR_t = \sum_{i=1}^{N_p} R_{it} \tag{3}$$

Local patch recruitment at time t depended on adult densities at *t-1* and followed a reparameterized Beverton-Holt function:

$$R_{it} = \frac{\alpha_i N_{it-1}}{1 + \frac{\alpha_i - 1}{\beta_i} N_{it-1}} \tag{4}$$

where α_i is the recruitment compensation ratio and β_i is local patch carrying capacity.

Management often monitors metapopulation resources as the aggregate of all local populations. For example, take a two patch metapopulation model that varies α_i and β_i parameters where:

```
alpha <- c(2, 4)
beta <- c(100, 200)
```

Here, recruitment compensation from local patches α_i gets averaged across the metapopulation leading to an average compensation ratio $\bar{\alpha}$ of 3. Likewise, the total carrying capacity of the metapopulation $\bar{\beta}$ becomes the summation of local patch carrying capacities $\sum \beta_i$, which is 300. This scale of monitoring generates the following local patch and metapopulation dynamics:

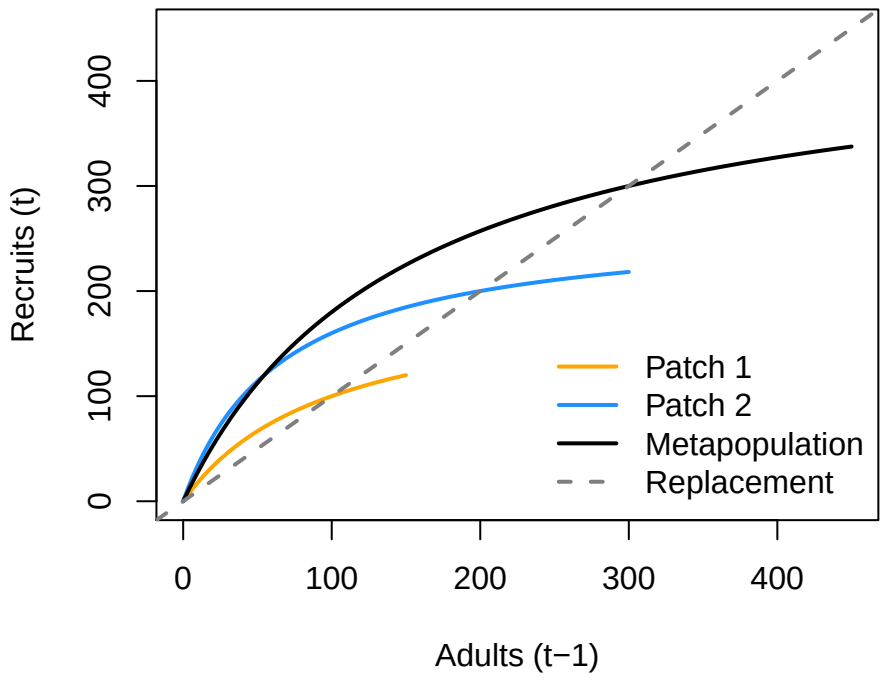

Figure S1: Metapopulation and local patch recruitment dynamics.

Creating the spatial networks

The next aspect to our metapopulation model is connecting the set of patches to one another (Yeakel et al. 2014). We need to specify the number of patches, their arrangements (i.e., connections), and how far apart they are from one another. We followed some classic metapopulation and source-sink arrangements to create four networks that generalize across a few real-world topologies: a linear habitat network (e.g., coastline), a dendritic or branching network (e.g., coastal rivers), a star network (e.g., mountain & valley, or lake with inlet tributaries), and a complex network (e.g., grasslands).

To make networks comparable, each spatial network type needs the same leading parameters (e.g., number of patches N_p and mean distance between neighboring patches $\bar{d}$). In this case, we set N_p to `16` and $\bar{d}$ to `1` unit (distance units are arbitrary). We used the `igraph` package (Csardi & Nepusz 2006) and some custom code to arrange our spatial networks as the following:

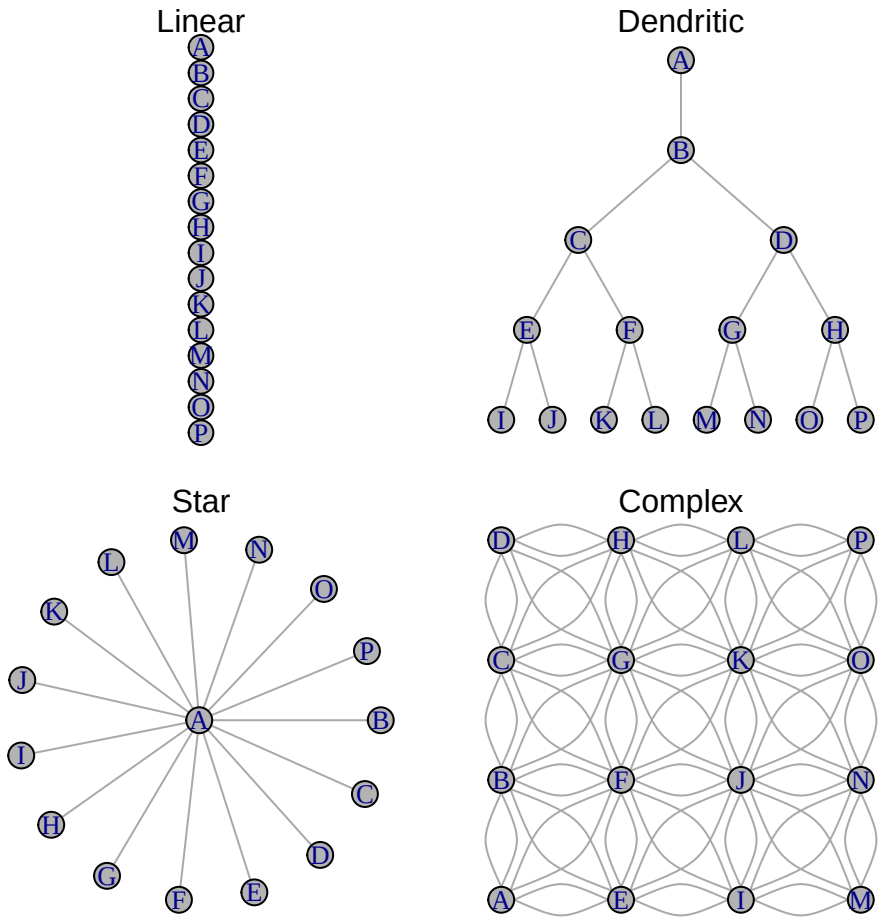

Figure S2: Four spatial network topologies.

Note that distances between neighbor patches in the above networks are equal.

An example dispersal matrix for the complex network:

```
##   A B E F C G D H I J K L M N O P
## A 0 1 1 1 2 2 3 3 2 2 2 3 3 3 3 3
## B 1 0 1 1 1 1 2 2 2 2 2 2 3 3 3 3
## E 1 1 0 1 2 2 3 3 1 1 2 3 2 2 2 3
## F 1 1 1 0 1 1 2 2 1 1 1 2 2 2 2 2
## C 2 1 2 1 0 1 1 1 2 2 2 2 3 3 3 3
## G 2 1 2 1 1 0 1 1 2 1 1 1 2 2 2 2
## D 3 2 3 2 1 1 0 1 3 2 2 2 3 3 3 3
## H 3 2 3 2 1 1 1 0 3 2 1 1 3 2 2 2
## I 2 2 1 1 2 2 3 3 0 1 2 3 1 1 2 3
## J 2 2 1 1 2 1 2 2 1 0 1 2 1 1 1 2
## K 2 2 2 1 2 1 2 1 2 1 0 1 2 1 1 1
## L 3 2 3 2 2 1 2 1 3 2 1 0 3 2 1 1
## M 3 3 2 2 3 2 3 3 1 1 2 3 0 1 2 3
## N 3 3 2 2 3 2 3 2 1 1 1 2 1 0 1 2
## O 3 3 2 2 3 2 3 2 2 1 1 1 2 1 0 1
## P 3 3 3 2 3 2 3 2 3 2 1 1 3 2 1 0
```

Dispersal

Dispersal from patch i into patch j depends on constant dispersal rate ω (defined as the proportion of total local recruits that will disperse) and an exponential distance-decay function between i and j with distance cost to dispersal m following Anderson et al. (2015):

$$E_{ij(t)} = \omega R_{it} p_{ij} \tag{5}$$

where E_{ij} is the total dispersing animals from patch i into patch j resulting from dispersal rate ω, total number of local recruits R_{it}, and probability of dispersal between patches p_{ij}:

$$p_{ij} = \frac{e^{-md_{ij}}}{\sum_{\substack{j=1 \\ j \neq i}}^{N_p} e^{-md_{ij}}} \tag{6}$$

where d_{ij} is the pairwise distance between patches, m is the distance cost to dispersal. The summation term in the denominator normalizes the probability of moving to any patch to between 0 and 1 with the constraint that dispersers cannot move back into their home patch (i.e., $j \neq i$. With $\bar{d} = 1$, $m = 0.5$, $\omega = 0.1$, $R_{it} = 100$ in a linear network:

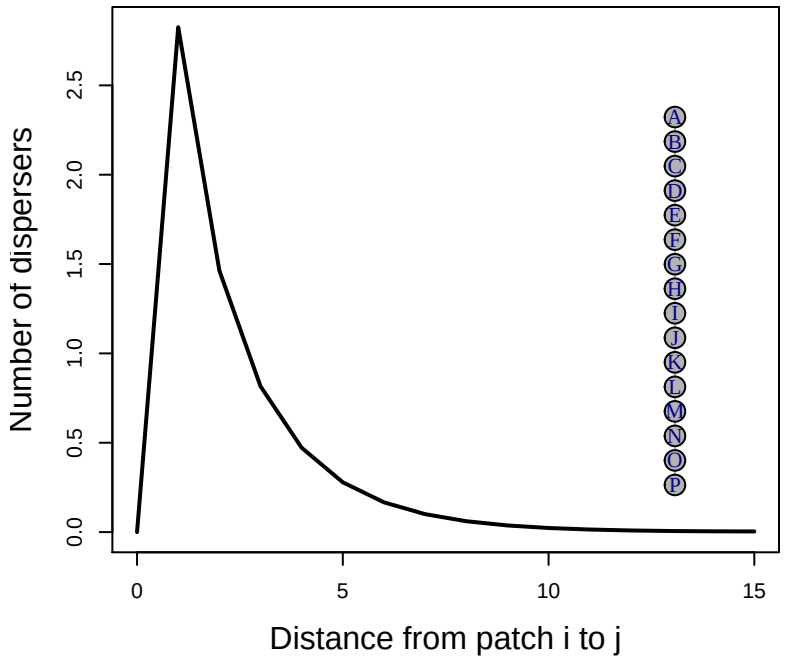

Figure S3: Example dispersal patterns across linear network.

Disturbance regimes

In all scenarios, disturbance was applied after `50` years of equilibrating the metapopulaton at pristine conditions. We then applied the disturbance regime at year `50` (the regime varied from *uniform*, *localized, random*, and *localized, extirpation* - see *Scenarios* below). Disturbance immediately removes a set proportion of the metapopulation adults at that time (i.e., `0.9` of $MN_{t=50}$). Once applied, the metapopulation was no longer disturbed and spatio-temporal recovery dynamics emerged naturally from these new conditions.

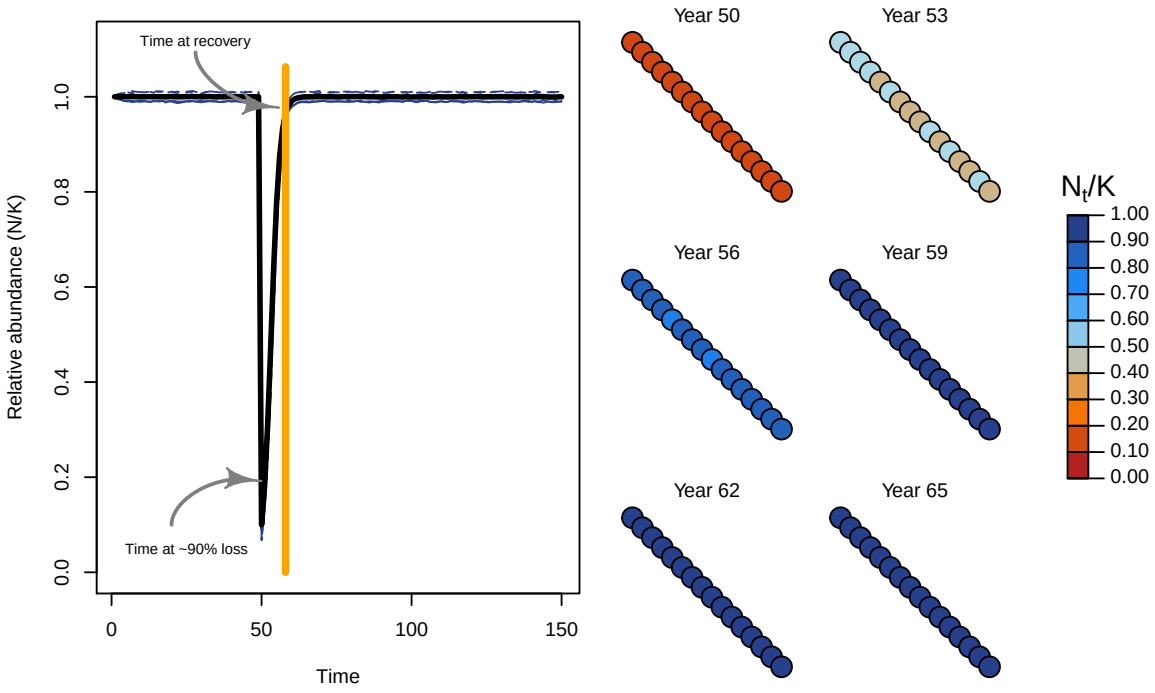

Figure S4: Recovery regime of metapopulation with linear topology through time (left) and space (right).

Recruitment stochasticity

Our model allowed for stochastic recruitment that followed a lognormal distribution with average variation in recruitment of σ_R. In cases of stochastic recruitment, the expected recruitment:

$$R_{it} = \frac{\alpha_i N_{it-1}}{1 + \frac{\alpha_i - 1}{\beta_i} N_{it-1}} \tag{7}$$

becomes:

$$R_{it} = \frac{\alpha_i N_{it-1}}{1 + \frac{\alpha_i - 1}{\beta_i} N_{it-1}} e^{(\epsilon_{it} - \frac{ln(\sigma_R^2 + 1)}{2})} \tag{8}$$

where lognormal deviates for each patch i at time t are drawn from a multivariate normal distribution (MVN) If σ_R is low, then metapopulation dynamics approach the deterministic case. In some scenarios, we evaluated the role of spatially and/or temporally correlated deviates across local patches to model potential common drivers affecting metapopulation dynamics (e.g., Moran effects). Expected recruitment deviates followed a first-order autoregression model such that:

$$\epsilon_{it} = \rho_T \epsilon_{t-1} + MVN(\mu = 0, \Sigma = \sigma_R(1 - \rho_T^2) e^{(-\rho_S D_{ij})}) \tag{9}$$

where ρ_T is temporal correlation (bounded $0-1$) ρ_S is rate of distance-decay in spatial correlation (bounded $0-\infty$ with higher values leading to independent patches). If rho_T is 0 and rho_S is high, then annual recruitment deviates are independent. We illustrate the effects of four kinds of recruitment deviates below using the same random number generator seed:

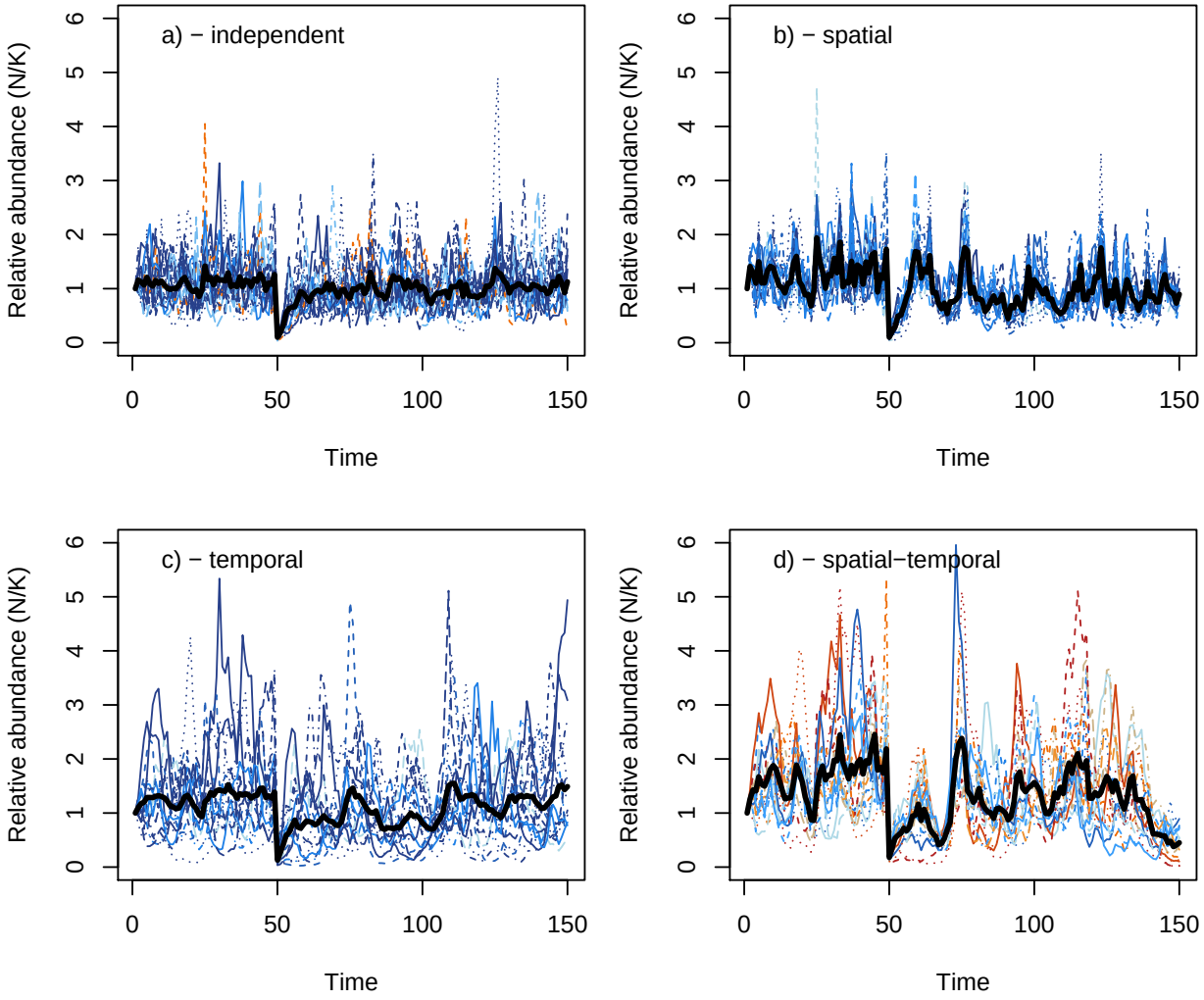

Figure S5: Metapopulation dynamics with independent (a), spatially correlated (b), temporally correlated (c), and spatio-temporally correlated (d) recruitment deviates. Black line indicates metapopulation, and dashed lines indicate local patches with red and blue relating to abundances after 100 years post-disturbance were less than or greater than 1.0 pre-disturbance, respectively.

Post-disturbance outcomes

We measured the following post-disturbance outcomes to track the temporal and spatial recovery regime of the metapopulation.

1. Collapse (a) & recovery rate (b) after disturbance:
    a. Collapse rate is defined as the number of simulations where metapopulation abundance failed to recover to `1.0` of the average pre-disturbance abundance for `5` consecutive years post-disturbance. This "collapse rate" reflects the risk of a long-term state shift in metapopulation dynamics after

disturbance in the face of stochasticity.

b. Recovery rate the number of years to average pre-disturbance abundance for `5` consecutive years. The recovery rate (either in the number of generations or in the rate of recovery per year) captures how quickly the aggregate metapopulation recovers from disturbance but doesn't take into account whether any given local patches recover to their pre-disturbance capacity.

2. Patch occupancy - the mean number of patches with `>0.1` local carrying capacity after disturbance in the short-term (5 years), medium-term (10 years), and long-term (25 years). This value characterizes the expected risk of spatial contractions or local patch collapses, and reflects how interactions between spatial structure, disturbance, and dispersal shape source-sink dynamics and the ability to provide (or not) rescue effects and recover local patches.

3. The ratio of expected maximum surplus production (we term MSY) to true maximum surplus production summed across all patches from fitted stock-recruitment model to aggregate across metapopulation such that:

$$\Delta_{MSY} = \frac{M\hat{S}Y_M}{\sum_{i=1}^{N_p} MSY_i} \tag{10}$$

A value of 1.0 would indicate that the disturbed metapopulation can sustain itself against the same disturbance regime as the sum of each patch independently. In other words, is the metapopulation more than (Δ_{MSY}>1.0), less than (Δ_{MSY}<1.0), or equal to the sum of its parts (Δ_{MSY}=1.0). We detail how MSY is estimated further below.

Monitoring & management at aggregate-scale

While true metapopulation dynamics are controlled by local patch dynamics and dispersal such that:

$$N_{it} = R_{it}\epsilon_{it} + I_{it} - D_{it} - E_{it} \tag{11}$$

$$R_{it} = \frac{\alpha_i N_{it-1}}{1 + \frac{\alpha_i - 1}{\beta_i} N_{it-1}} \tag{12}$$

$$MN_t = \sum_{i=1}^{N_p} N_{it} \tag{13}$$

$$MR_t = \sum_{i=1}^{N_p} R_{it} \tag{14}$$

Natural resoure managers often monitors and manages at the scale of the metapopulation. Hence, management at this scale inherently defines the stock-recruitment dynamics of the aggregate complex of patches (i.e., metapopulation) as:

$$MR_t = \frac{\hat{\alpha_t} MN_{t-1}}{1 + \frac{\hat{\alpha_t} - 1}{\hat{\beta_t}} MN_{it-1}} \tag{15}$$

where $\hat{\alpha_t}$ is the estimated compensation ratio averaged across the metapopulation at time t and $\hat{\beta}_t$ is the estimated carrying capacity of the entire metapopulation. Necessarily, these estimates emerge from monitoring data collected across all patches and are sensitive to the quality of the data and how local patches perform through time. For example, temporal shifts in productivity regimes may be masked if most of the data were sampled before the regime shift. To help surmount these issues, modern resource assessments use data weighting and penalties (i.e., priors) when fitting models to data.

In our assessment, we weighted recent years of sampling over more distant years such that:

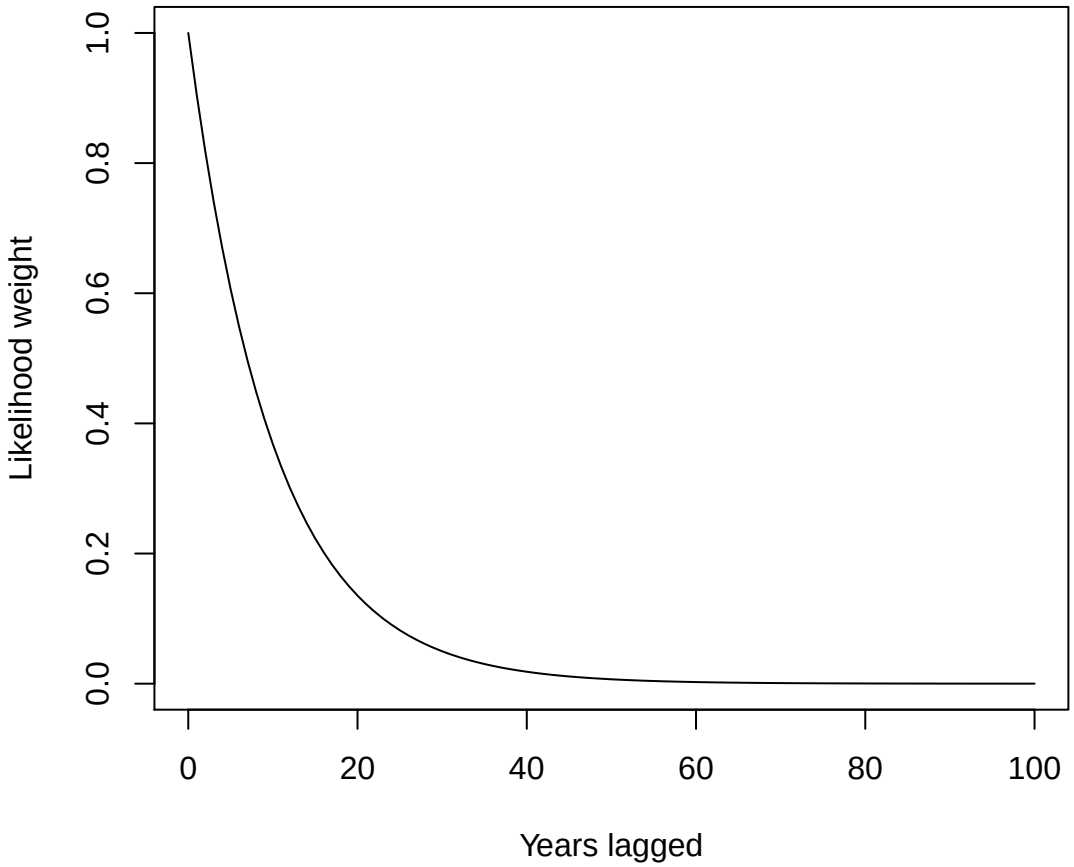

Figure S6: Likelihood weighting for samples collected over time from current year of sampling.

This forward-weighting approach increased the sensitivity of the monitoring sub-model to detect demographic changes in the post-disturbance recovery regime. Data-weighting is increasingly being used in resource monitoring, although how weights are developed and applied to data is a case-by-case basis.

Furthermore, we used penalized normal likelihoods on both $\hat{\alpha_t}$ and $\hat{\beta}_t$ such that:

$$\hat{\alpha_t} \sim N(\mu = \hat{\alpha_{t-1}}, \sigma = 3\hat{\alpha_{t-1}}) \tag{16}$$

and

$$\hat{\beta}_t \sim N(\mu = \hat{\beta_{t-1}}, \sigma = 3\hat{\beta_{t-1}}) \tag{17}$$

where $\mu = \hat{\alpha_{t-1}}$ and $\mu = \hat{\beta_{t-1}}$ represents the best estimates from the previous assessment and the `3` in the σ term represents a 300% coefficient of variation. We used these penalized likelihoods to fit the above aggregate stock-recruitment model with *lognormal* error to the metapopulation stock-recruit data collected at time t. We used the following function and fitted to the below θ parameters (termed `theta` in the function `optim()` using the `L-BFGS-B` optimizer with a lower bound on $\hat{\alpha}$ of `1.01` (i.e., constrained to be at least above replacement).

```
SRfn <- function(theta, data, lastYr) {
    a.hat <- theta[1]
    b.hat <- exp(theta[2])
    sd.hat <- exp(theta[3])
    rec.mean <- (a.hat * data$spawners)/(1 + ((a.hat - 1)/b.hat) * data$spawners)
    # negative log likelihood on recruitment parameters
    nll <- -1 * sum(dlnorm(data$recruits, meanlog = log(rec.mean), sdlog = sd.hat,
        log = TRUE) * data$weights, na.rm = TRUE)
    # penalized likelihood on estimated alpha
    penalty1 <- -dnorm(a.hat, lastYr$alphaLstYr, 4 * lastYr$alphaLstYr, log = TRUE)
    # penalized likelihood on estimated carrying capacity
    penalty2 <- -dnorm(b.hat, lastYr$metaKLstYr, 4 * lastYr$metaKLstYr, log = TRUE)
    jnll <- sum(c(nll, penalty1, penalty2), na.rm = TRUE)
    return(jnll)
}
```

This above function allows us to assess the bias in $\hat{\alpha_t}$, $\hat{\beta}_t$, and $\hat{MR_t}$ compared to true $\bar{\alpha}$, $\bar{\beta}$, and MR_t across the metapopulation. This then allows us to see how much information management & monitoring programs are missing when they assess metapopulations at the aggregate (rather than local) scales.

Finding maximum sustainable yield

Resource managers measure productivity with a variety of performance reference points (Forrest et al. 2010). One of the most widely used metrics, commonly called *Maximum Sustainable Yield* in fisheries and other harvest literature (MSY), relates to the largest loss the population can sustain over an indefinite period of time while maximizing its ability to replenish itself. Under density-dependent growth, individuals' growth, survival, and reproduction at low population densities are not constrained by limited resources, but overall production is low because there are few individuals. At high densities, limited resources increasingly constrain individual's reproductive success until the population reaches carrying capacity, and overall production drops to zero because per-capita success is low. However, at some intermediate densities, both per-capita and overall production is high, and population growth is at its maximum point due to the large number of reproducing individuals. At this point, there is the maximum surplus of individuals produced above replacement that can help to withstand disturbance or harvest regimes and contribute to future recovery, either through increasing local patch densities or by emigrating neighboring patches providing "rescue effects".

Under Beverton-Holt or Ricker density-dependent recuitment, however, there exists no analytical solution for calculating MSY. Therefore, we used numerical methods and a one dimensional root finder to iteratively search for the population mortality that maximized surplus production in the metapopulation. We term this mortality F_{MSY} and can use this mortality value to calculate maximum surplus production MSY, the adult densities that produce MSY (termed N_{MSY}), and the recruits that result from this (termed R_{MSY}).

```
# uniroot numerical search

yieldRoot <- function(alpha, beta, Fcur, model) {
```

```
    Ucur <- 1 - exp(-Fcur)
    if (model == "Beverton-Holt") {
        # population model is R ~ (CR * S)/(1+(CR-1)/K * S): reparameterized
        # Beverton-Holt
        adults <- beta * exp(-Fcur)
        recruits <- (alpha * adults)/(1 + ((alpha - 1)/beta) * adults)
        yield <- recruits - adults
    }
    if (model == "Ricker") {
        # population model is R ~ CR * S * e(-log(CR)/K * S): reparameterized Ricker
        adults <- beta * exp(-Fcur)
        recruits <- alpha * adults * exp((-log(alpha)/beta) * adults)
        yield <- recruits - adults
    }
    return(list(recruits = recruits, adults = adults, yield = yield))
}

# Return approximate gradient for integral

fun_yield <- function(Fcur, alpha, beta, delta, model) {
    y1 <- yieldRoot(alpha = alpha, beta = beta, Fcur = Fcur - delta/2, model = model)$yield
    y2 <- yieldRoot(alpha = alpha, beta = beta, Fcur = Fcur + delta/2, model = model)$yield
    approx.gradient <- (y2 - y1)/delta
    return(approx.gradient)
}

# uniroot search for optimal yield and Fmsy
findMSY <- function(alpha, beta, Npatches, model) {
    F_msy <- NULL
    for (i in 1:Npatches) {
        a_p <- alpha[i]
        b_p <- beta[i]
        F_msy[i] <- uniroot(fun_yield, interval = c(0, 1), extendInt = "yes",
            alpha = a_p, beta = b_p, delta = 1e-04, model = model)$root
    }
    MSY <- sapply(1:Npatches, function(x) {
        yieldRoot(alpha = alpha[x], beta = beta[x], Fcur = F_msy[[x]][1], model = model)
    })
    return(list(F_msy = F_msy, MSY = MSY))
}
```

Scenarios

We tested all combinations of the following eight processes (below) and ran `100` iterations per scenario to estimate the mean for each of the above outcomes.

1. Homogenous and spatially variable recruitment compensation ratio across patches, i.e. intrinsic rate of population growth (α_i).
2. Homogenous and spatially variable local carrying capacity across patches, i.e. asymptote of expected recruits at high adult densities (β_i)
3. Disturbances where a proportion of individuals removed from metapopulation (e.g., `0.90`) occurs.
    a. *uniform* - random individuals removed at equal vulnerability across all patches.

   b. *localized, random* - random individuals removed from randomly selected subset of patches (as long as the target individuals lost in the metapopulation can be achieved in that subset of patches)
   c. *localized, extirpation* - total extirpation of randomly selected subset of patches (as long as the target individuals lost in the metapopulation can be achieved in that subset of patches)

4. Density-independent dispersal rates ω from 0 to 20% of individuals within a patch will disperse.

5. Topology of the spatial networks with linear, dendritic, star, and complex networks. Each network with N_p of `16` and distance between patches $\bar{d}$ of `1`.

6. Stochastic recruitment deviates from low, medium, high coefficient of variation on lognormal error. Generate stochasticity in time-dynamics via random recruitement deviates away from expected.

7. Temporal correlation in recruitment deviates from low, medium, high correlation (i.e., good year at time t begets good year at time $t+1$).

8. Spatial correlation in recruitment deviates among patches from low, medium, to high correlation (i.e., neighboring patches go up or down together).

Example results

We demonstrate our metapopulation model with an example outcome for a linear network composed of `16` patches, a dispersal rate of `0.01` and a high enough dispersal cost such that individuals are only willing to move to their closest neighboring patches. This limits the strength of potential rescue effects. For this example, patches varied in their productivity and carrying capacity but will have deterministic population dynamics.

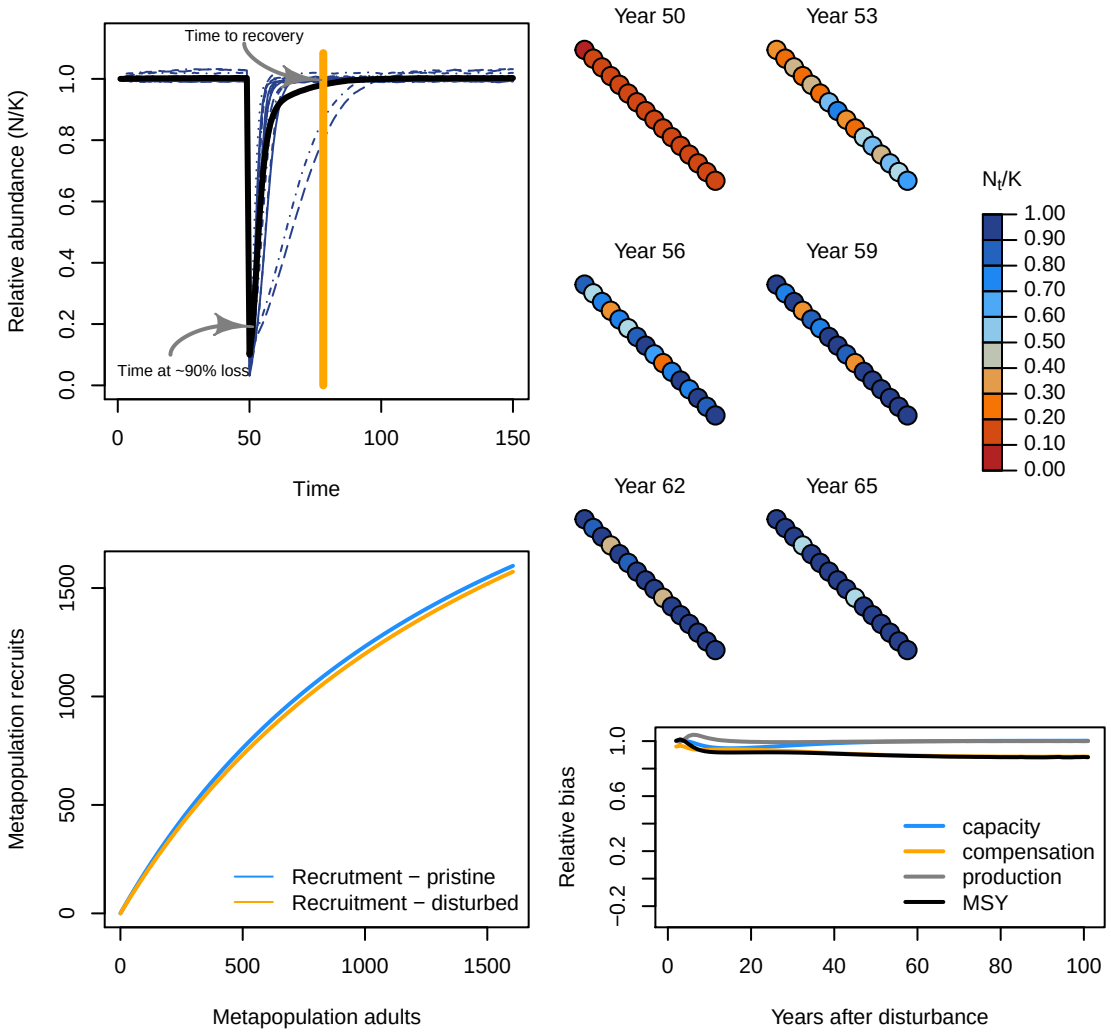

Figure S7: Example iteration of spatial recovery regime of metapopulation with linear topology through time (top left) and space (top right). Recruitment dynamics before and 10 years after disturbance (bottom left). Relative bias in aggregate-scale estimates of carrying capacity, compensation ratio, and recruitment production in recovery phase (bottom right).

210 We can then contrast this with a different network shape, like a dendritic network.

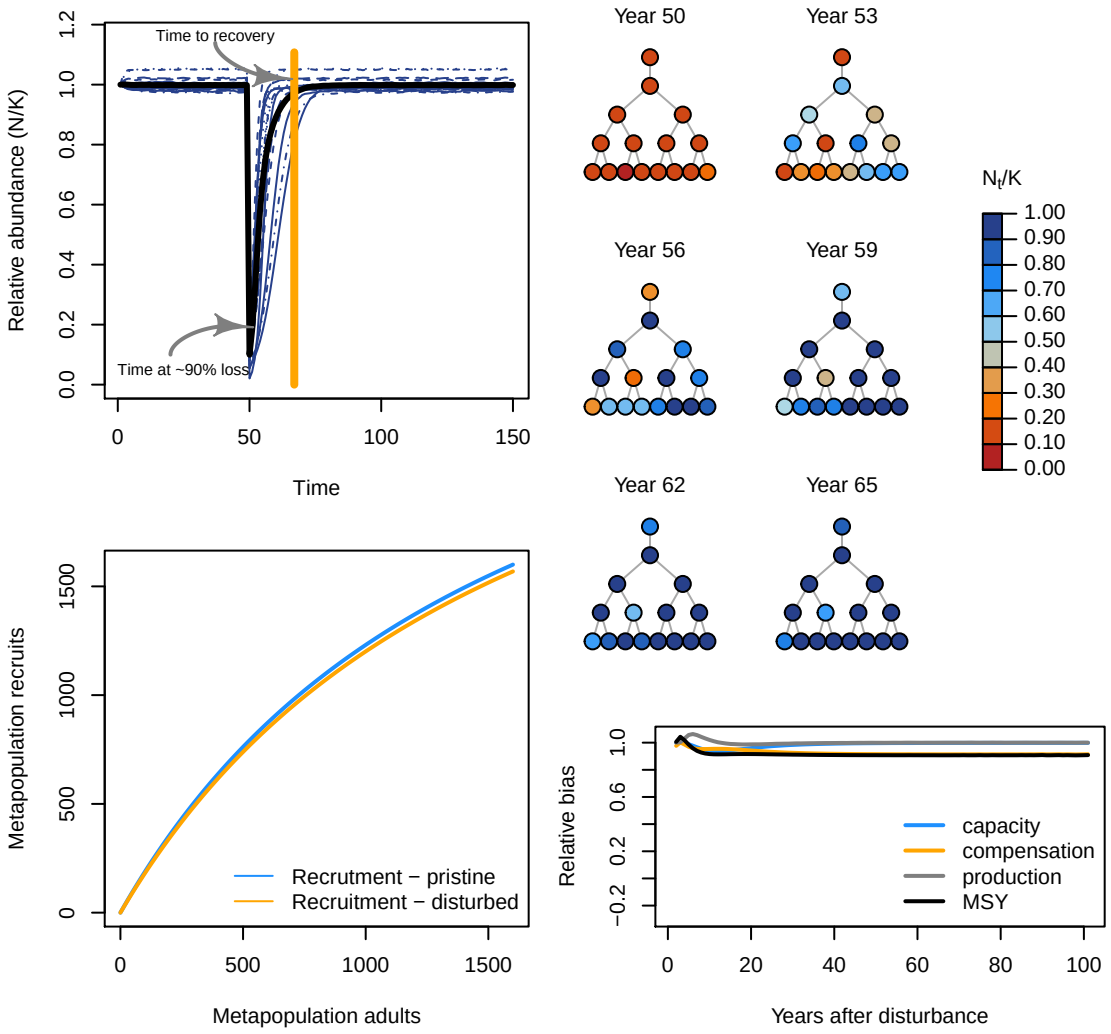

Figure S8: Example iteration of spatial recovery regime of metapopulation with dendritic topology.

211 Now, let's add some stochasticity to recruitment and see how this affects the recovery regime.

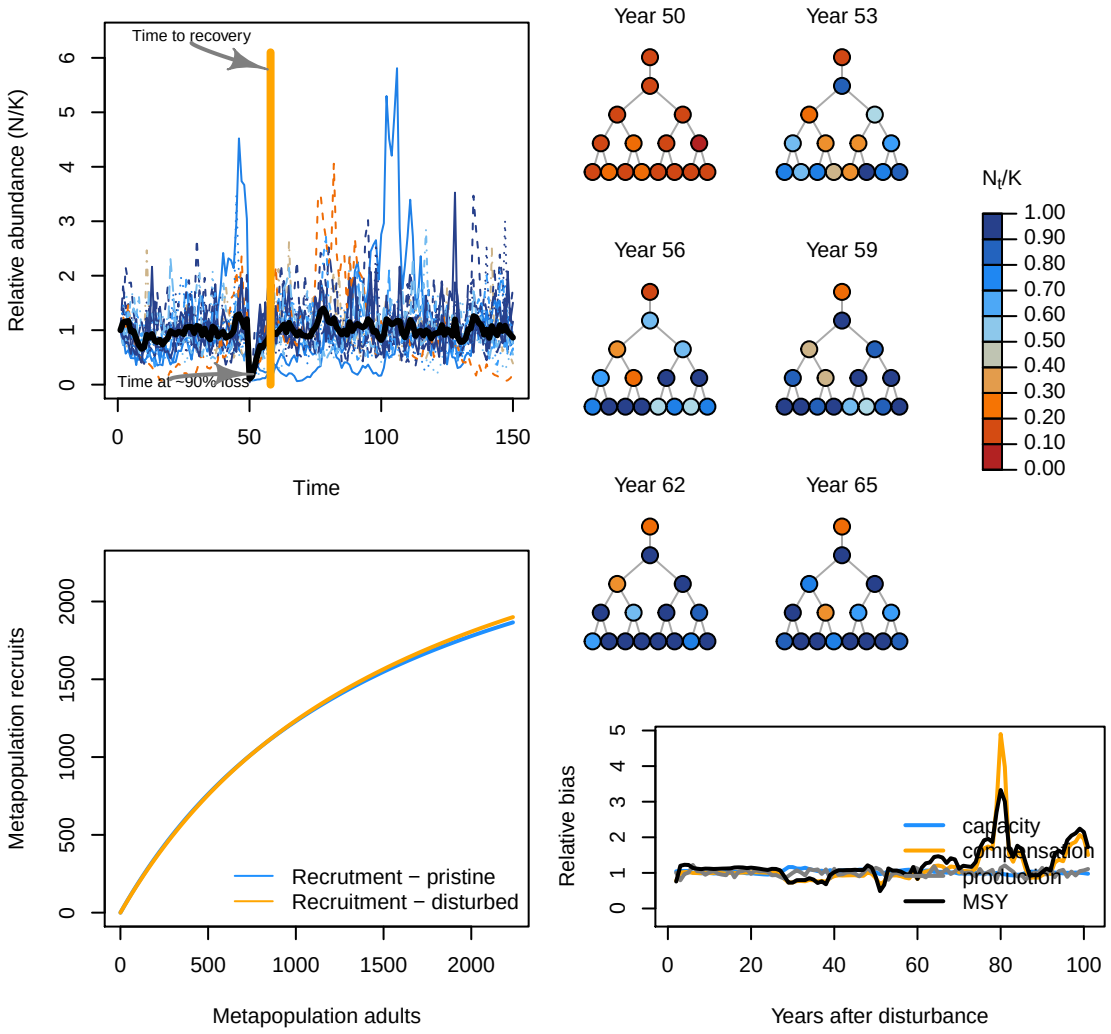

Figure S9: Example iteration of spatial recovery regime of stochastic metapopulation.

Next, we can contrast with a disturbance regime where the disturbance is concentrated on local patches that can be completely extirpated (rather than the disturbance being applied proportionally across all patches e.g., a mixed-stock fishery).

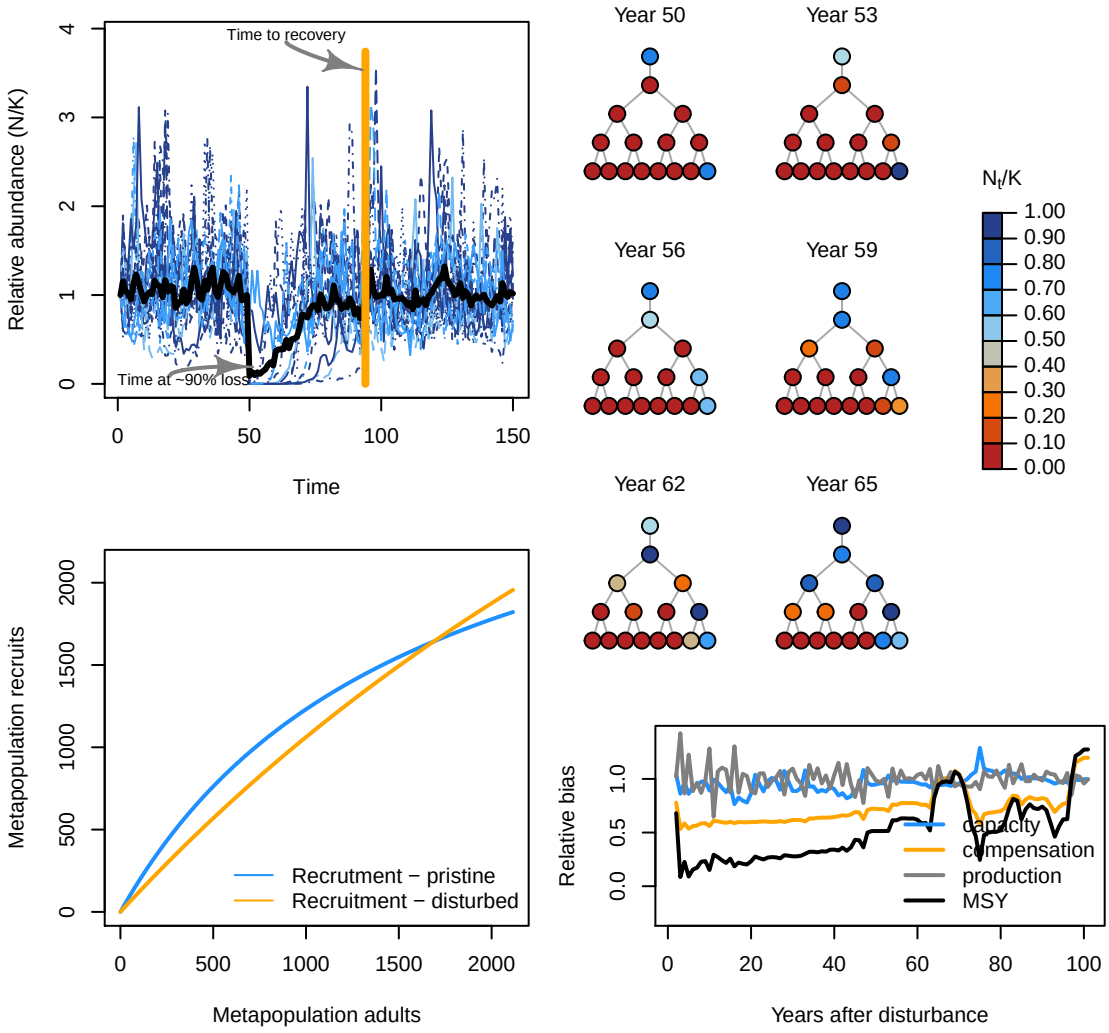

Figure S10: Example iteration of spatial recovery regime of stochastic metapopulation.

General patterns

Effects of disturbance regime

The strongest lever influencing recovery in our simulated metapopulations was by far, the characteristics of the disturbance regime. That is, more influential than the density dependence relationship, dispersal rates or network topology was how targeted patches were in the severity of disturbance. This was surprising and not expected in our initial hypotheses. Localized disturbances increased the risk of spatial contraction, reduced recovery rates and aggregate compensation, and increased the risk of a long-term state shift. By altering aggregate compensation, localized disturbance reduced the surplus production of the metapopulation. In other words, through changes in source-sink dynamics, metapopulations under localized disturbance acted less than the sum of their parts – the more localized the impacts, the worse these effects. Uniform disturbances generally left the metapopulation dynamics unaffected with few ecological surprises. These above spatial and temporal recovery processes also appeared tied to one another such that changes to any of them had feedbacks with other recovery metrics.

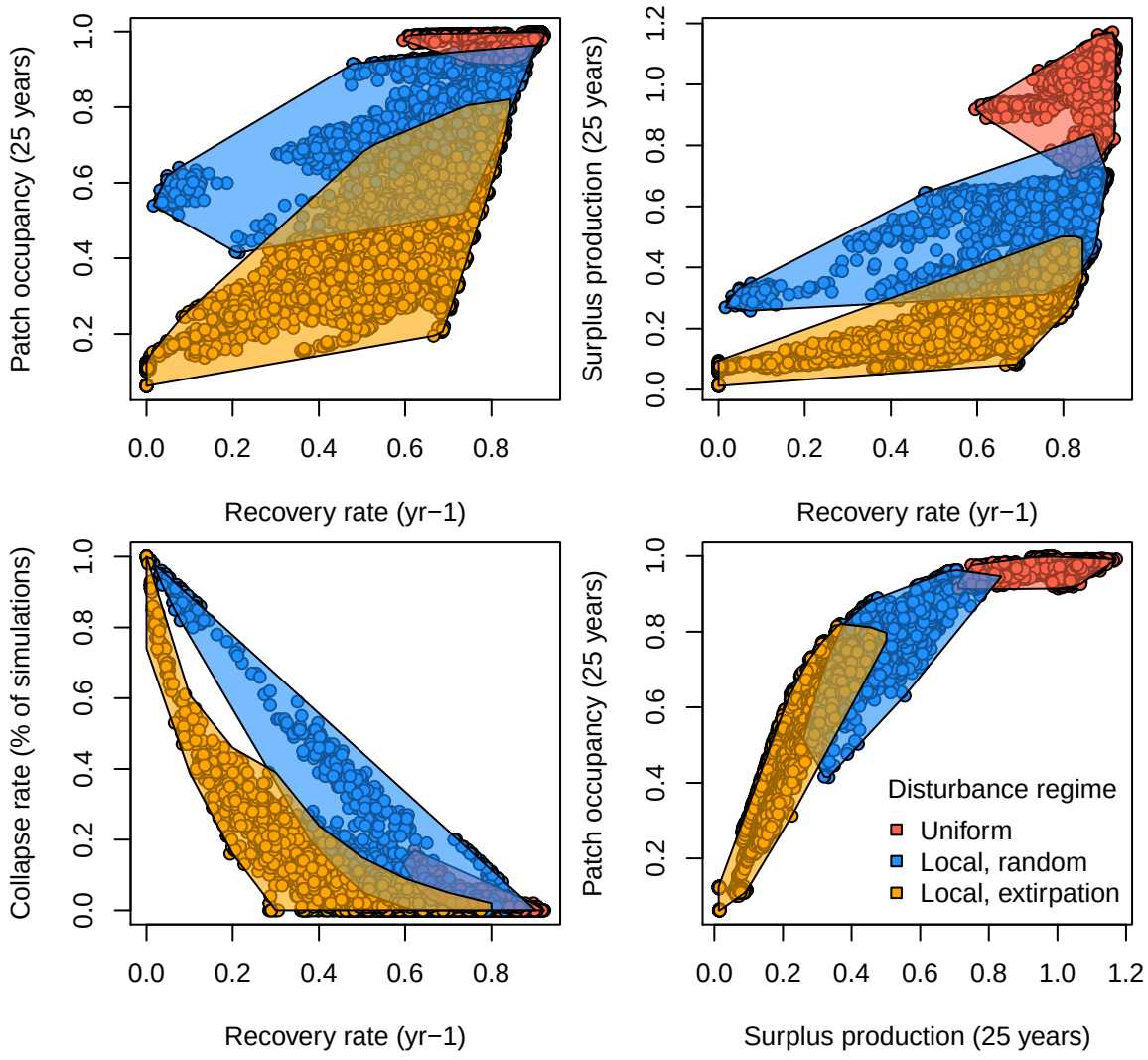

Figure S11: Spatial and temporal recovery patterns along disturbance regimes across all scenarios.

Role of network structure & dispersal

We now show some general patterns in how variable patch demographic rates, network structure, dispersal, disturbance, recruitment stochasticity, and spatio-temporal correlations variation affects metapopulation *recovery rates*, *maximum sustainable yield* (analagous to the maximum rate of loss the system can sustain), and *collapse rate* (i.e, the number of simulations where the metapopulation fails to recover), and *patch occupancy* (i.e., number of patches with local abundance above some baseline).

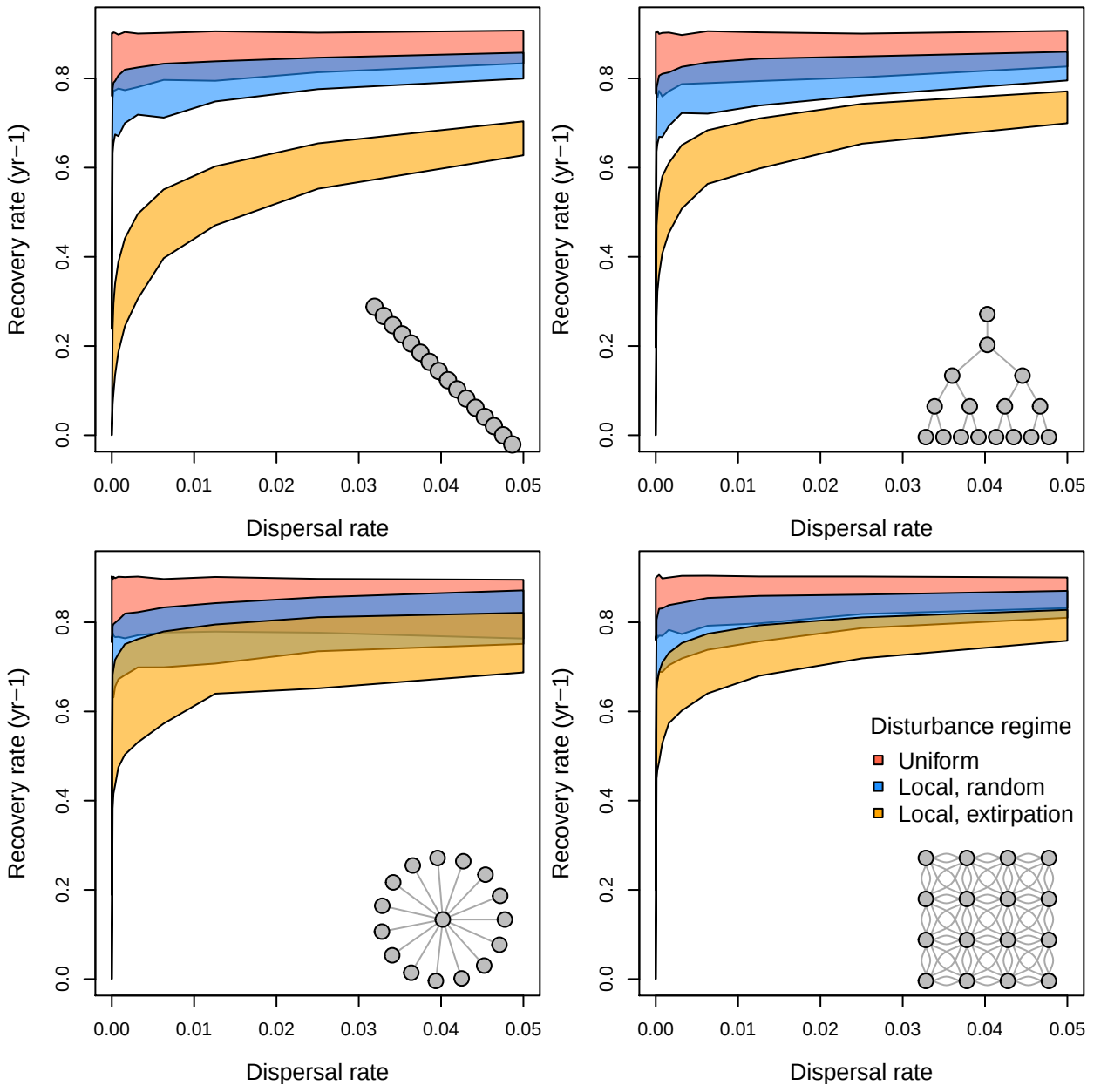

Figure S12: Metapopulation recovery rates along gradients of network configuration, dispersal rates, and spatial distribution of disturbance. The shaded region describes the interquartile range across all scenarios.

Dispersal, landscape structure, and local density-dependence also affected metapopulation recovery patterns in three key ways, though to a lesser extent. First, recovery rates increased with increased dispersal. However, this effect was nonlinear with diminishing benefits of dispersal occurring at ~1-3%, depending on

spatial structure and disturbance. Second, more linearized networks had slower recovery times than more connected networks suggesting that rescue effects take some time to cascade through the entire network of patches; but this interacted with the disturbance regime as only local, extirpation exhibited this change in any substantial manner. Last, diversity in local patch compensation and carrying capacities tended to slow metapopulation recoveries - this effect interacted with other factors like stochasticity.

Figure S13: Effects of variable local patch productivities on metapopulation recovery across all scenarios.

Patterns in recovery rates

First, lets show recovery rates for a scenario where (1) patches have the same local productivities and carrying capacities, (2) patches have different productivities and carrying capacities, (3) recruitment is deterministic and patches are different, and (4) spatial-temporal correlation in stochastic recruitment.

Below, we can see three main effects on recovery rates (number of generations to reach recovery). First, recovery gets faster with increased dispersal. Most of the action here takes place at low rates of dispersal indicating most spatial topologies don't need much dispersal to quicken their recovery. In preliminary runs, dispersal rates of `0.05-0.2` provided similar recovery patterns. Second, more localized disturbances regimes lead to slower recovery. Third, linearized networks have slower recovery times than interconnected, complex networks suggesting that rescue effects take some time to cascade through the entire network of patches.

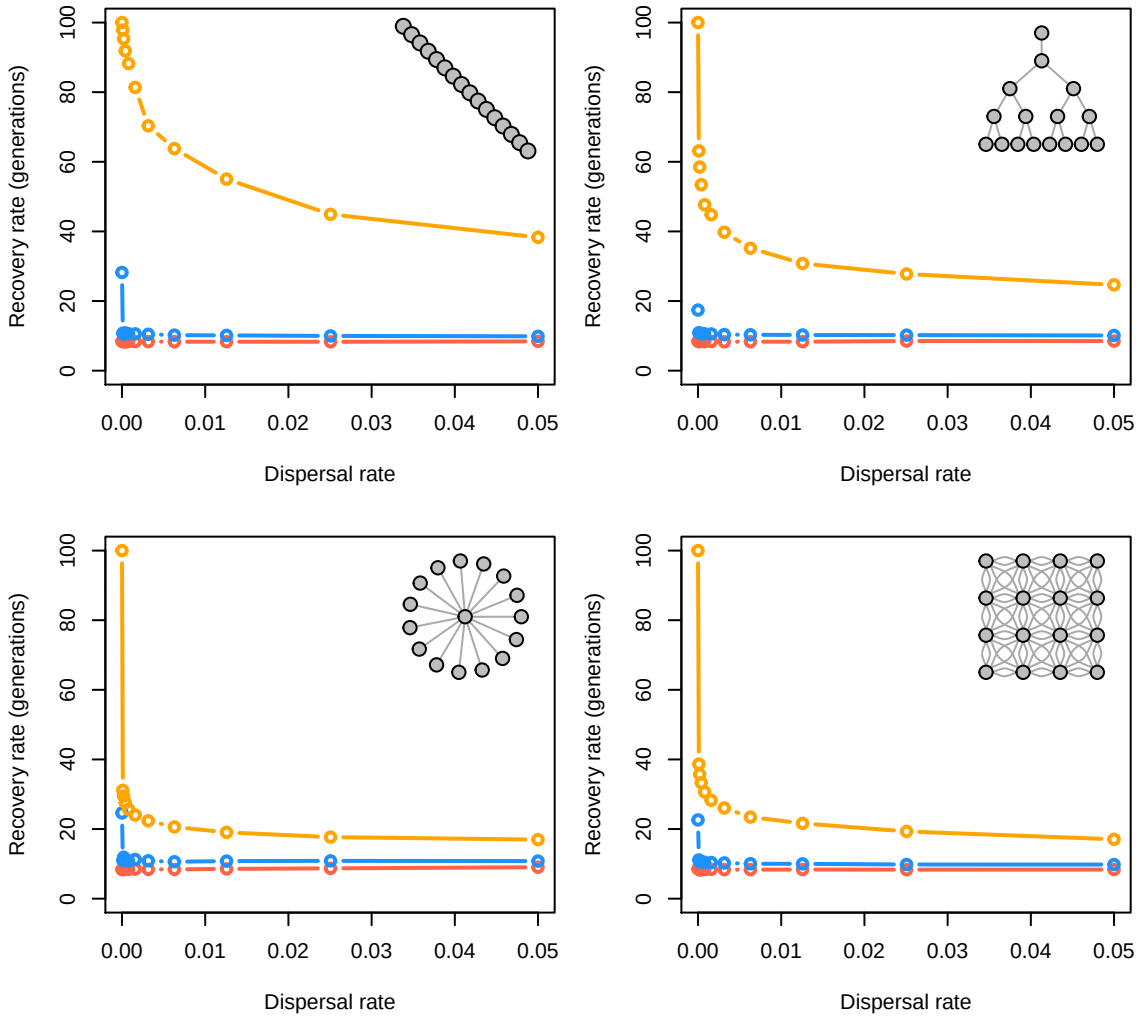

Figure S14: Recovery rates along dispersal, disturbance (red - uniform; blue - localized, random; orange - localized, extirpation), and network gradients without stochasticity.

Now, lets show recovery rates for the same scenario with deterministic recruitment but allowing for patches to vary in productivity and carrying capacity. In addition to the same three main effects of dispersal, network, and disturbance noted above, we also see variable patch productivities slows recovery across all scenarios.

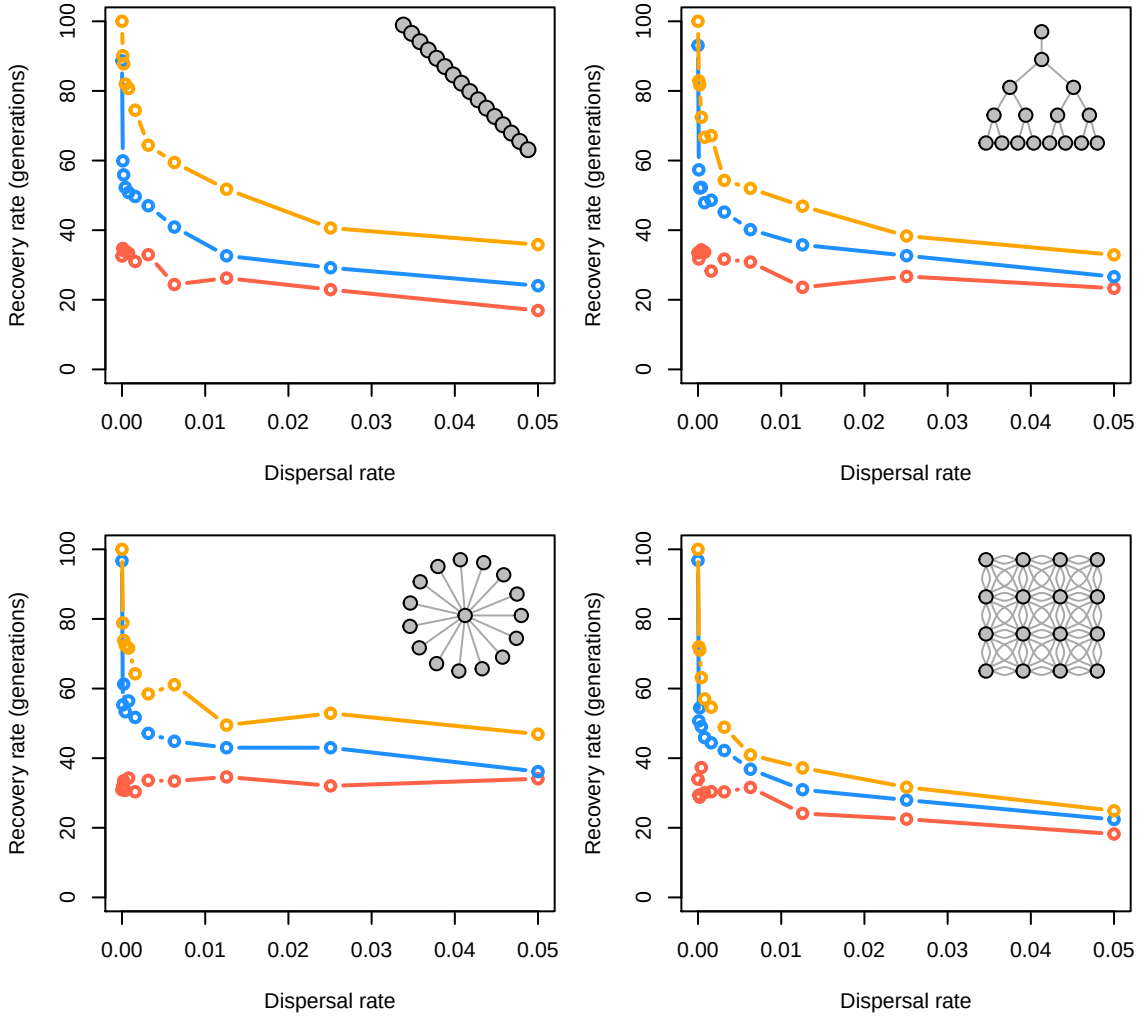

Figure S15: Recovery rates along dispersal, disturbance (red - uniform; blue - localized, random; orange - localized, extirpation), and network gradients with variable local productivity and carrying capacities.

Now, lets show recovery rates for the same scenario but allowing for recruitment to be stochastic (but patches are identical in demographic traits). We see the same three main effects of dispersal, network, and disturbance noted above. We also see a few subtle changes: (1) stochasticity slows recovery for uniform and local disturbance, but (2) quickens recovery for extreme local disturbance.

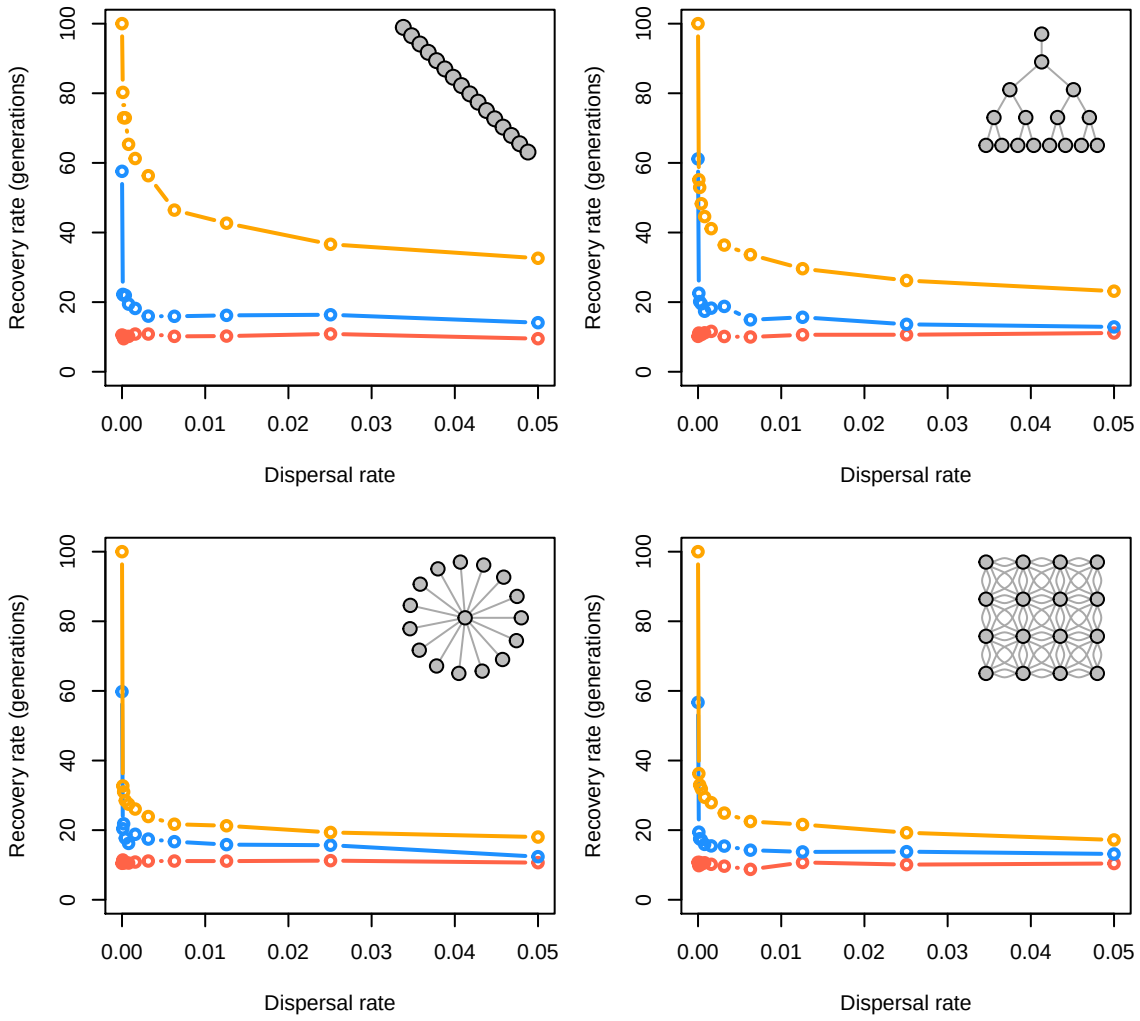

Figure S16: Recovery rates along dispersal, disturbance (red - uniform; blue - localized, random; orange - localized, extirpation), and network gradients with stochasticity.

Now, lets show recovery rates for the same scenarios but with spatial and temporal correlations in recruitment stochasticity. In addition to the same effects of stochasticity, we also generally see a small effect of slower recovery times for uniform and local disturbance, but faster recovery times for extreme localized disturbance.

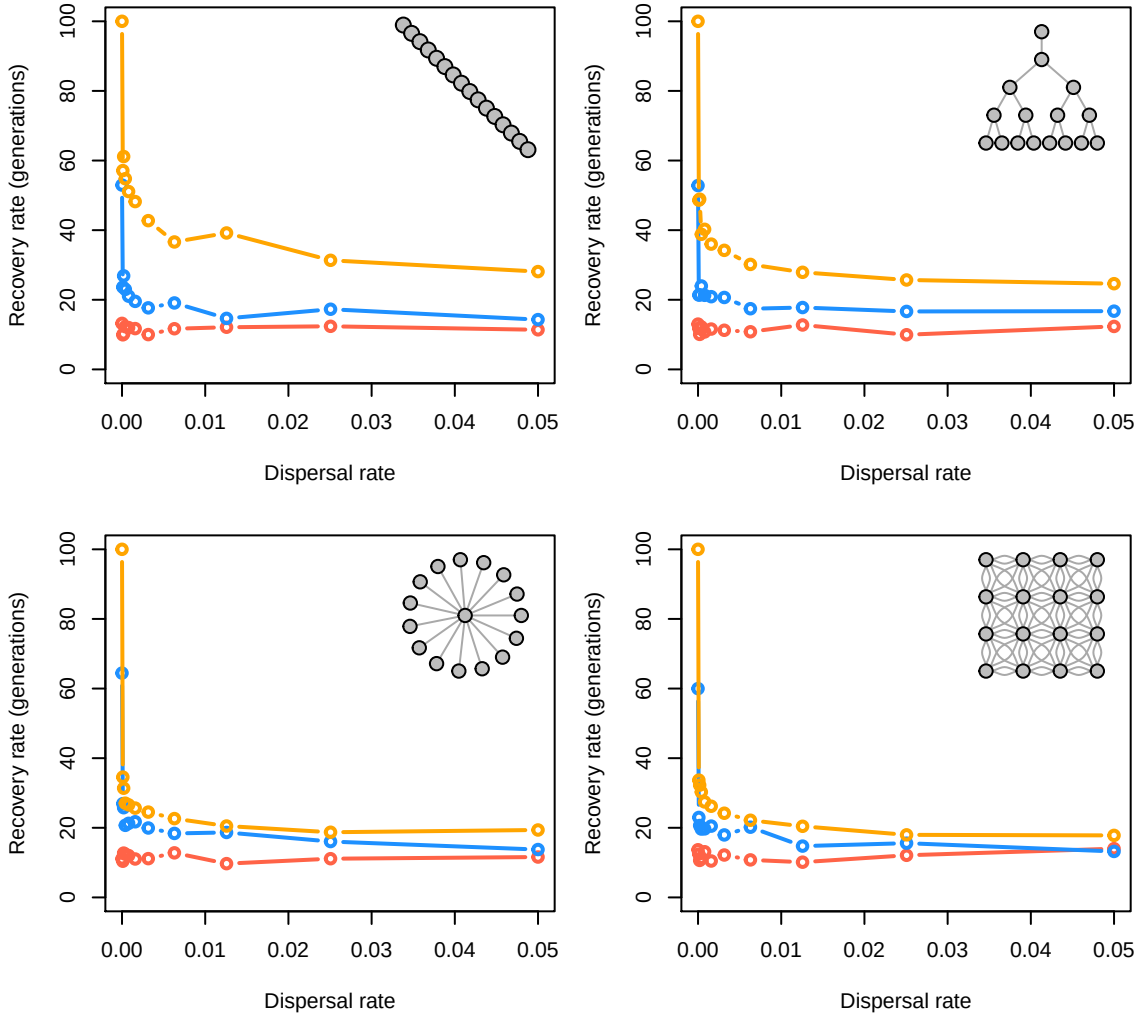

Figure S17: Recovery rates along dispersal, disturbance (red - uniform; blue - localized, random; orange - localized, extirpation), and network gradients with high spatial-temporal correlation in recruitment variation.

Patterns in MSY

MSY with deterministic recruitment where patches are the same

We now show similar patterns in how the maximum surplus production of the whole metapopulation (i.e., MSY) shifts in the first 25 years post-disturbance compared to the sum of MSY for each patch. A value of 1.0 would indicate that the disturbed metapopulation can sustain itself against the same disturbance regime as the sum of each patch independently. In other words, is the metapopulation more, less, or equal to the sum of its parts.

We will show 25-year MSY patterns for a scenario where (1) patches have the same local productivities and carrying capacities, (2) patches have different productivities and carrying capacities, (3) recruitment is deterministic and patches are different, (4) spatial-temporal correlation in stochastic recruitment.

Below, we can see two main effects on surplus production. First, spatial disturbance is a strong driver of surplus production with more localized disturbance reducing the surplus. Second, dispersal rates are only limiting in scenarios with localized disturbance. This suggests that (1) uniformly disturbed metapopulations operate as the "sum of their parts" but (2) localized disturbances affect metapopulation surplus production leading to slower internal recovery and/or reduced rescue effects from neighboring patches.

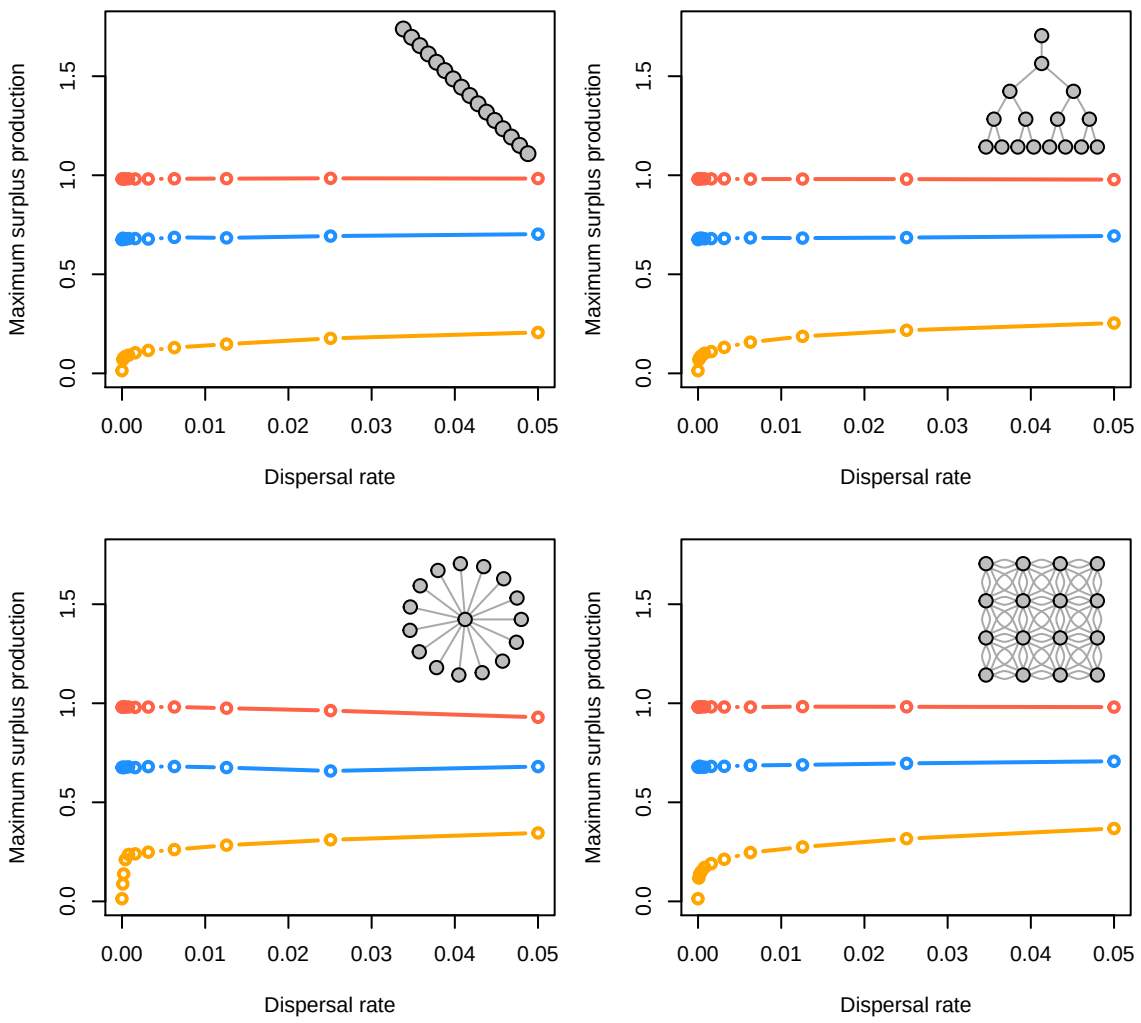

Figure S18: Maximum surplus production along dispersal, disturbance (red - uniform; blue - localized, random; orange - localized, extirpation), and network gradients with deterministic recruitment and the same patches.

277 **MSY with variable patches**

278 Now, we illustrate how variable patch demography affects the 25-year average MSY.

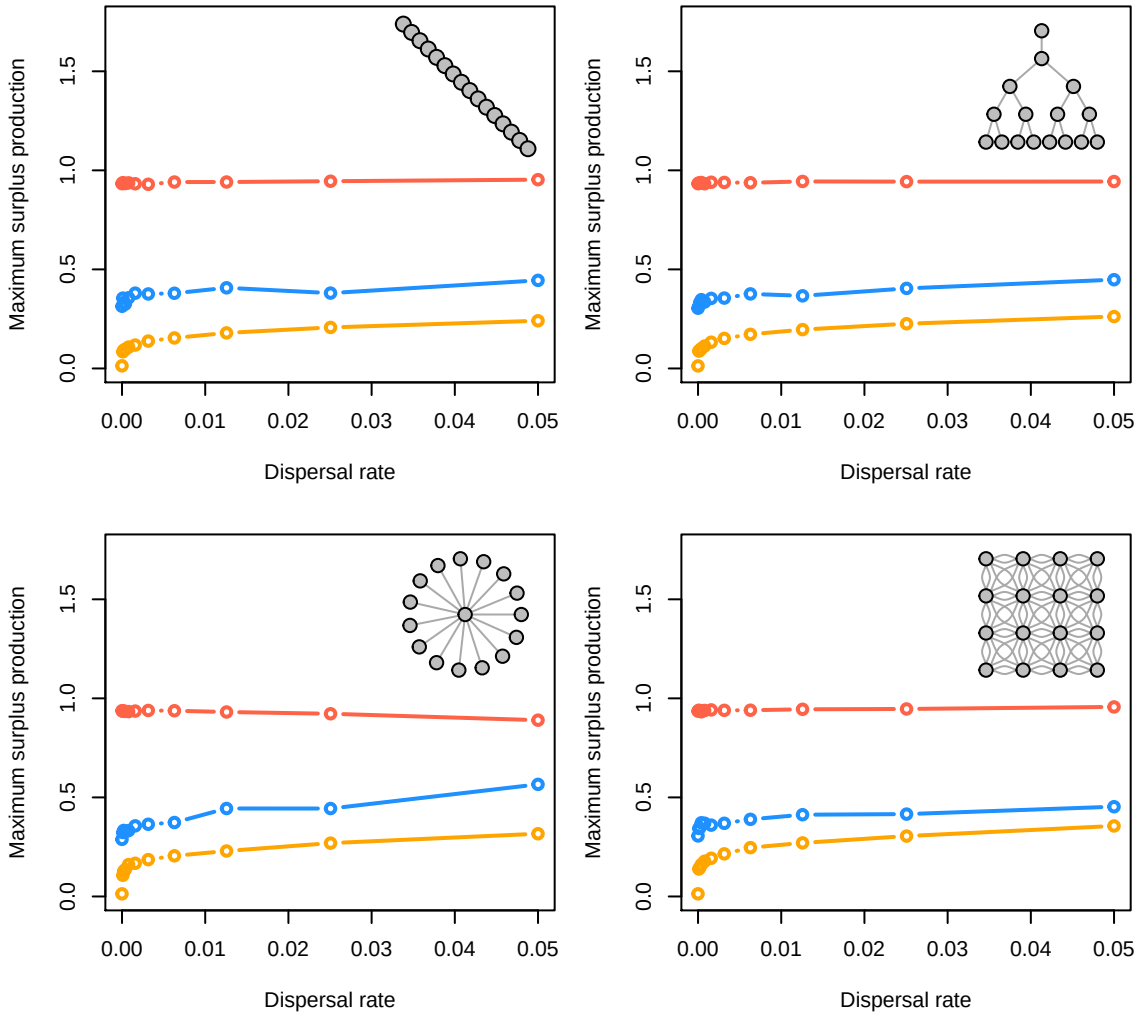

Figure S19: Maximum surplus production along dispersal, disturbance (red - uniform; blue - localized, random; orange - localized, extirpation), and network gradients with variable patches.

279 **MSY with variable patches and stochasticity**

280 Now, we illustrate how variable patch demography affects the 25-year average MSY.

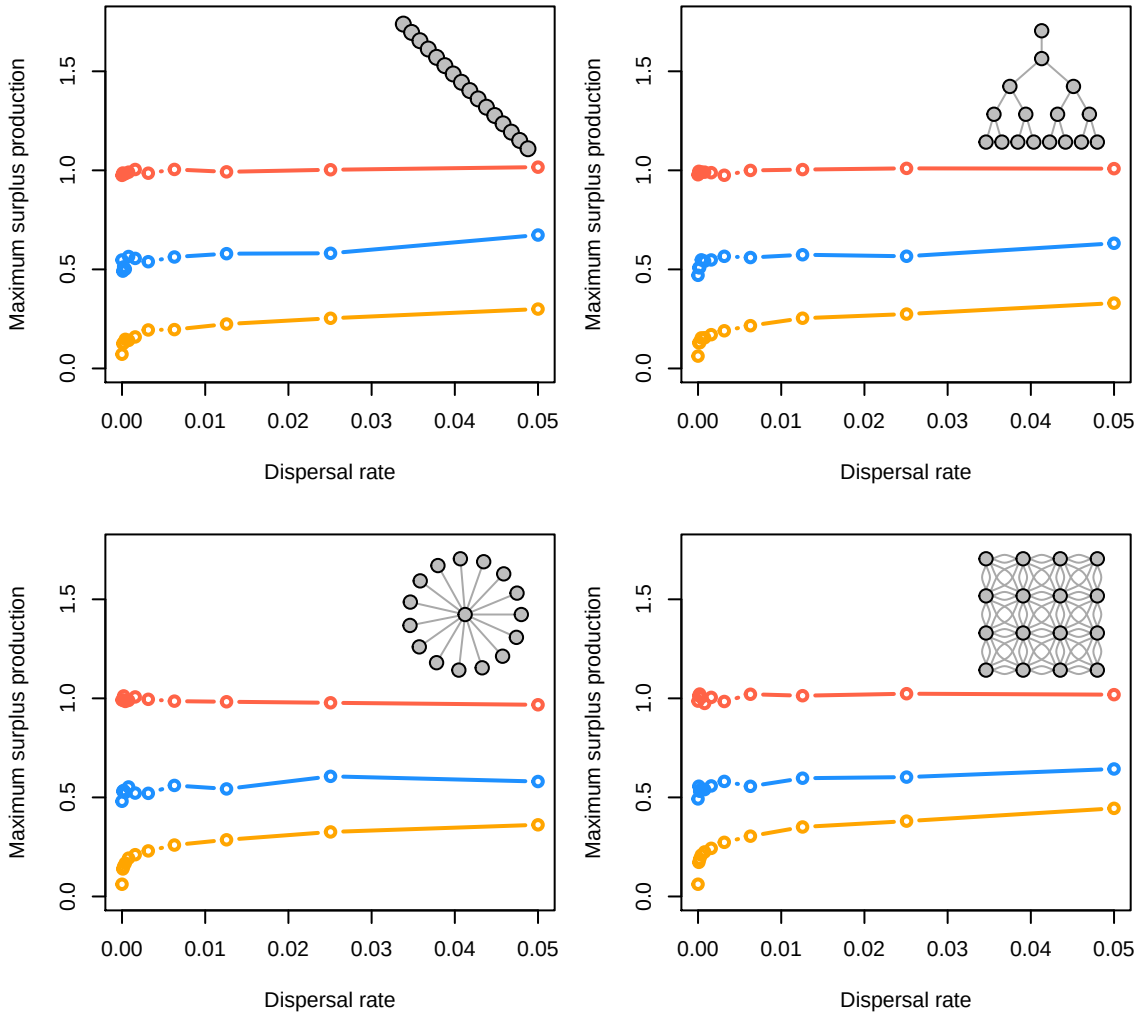

Figure S20: Maximum surplus production along dispersal, disturbance (red - uniform; blue - localized, random; orange - localized, extirpation), and network gradients with variable patches and stochasticity.

MSY with variable patches, and spatio-temporally correlated stochasticity

Now, we illustrate how variable patch demography and high spatial-temporal correlations in stochastic recruitment affects the 25-year average MSY.

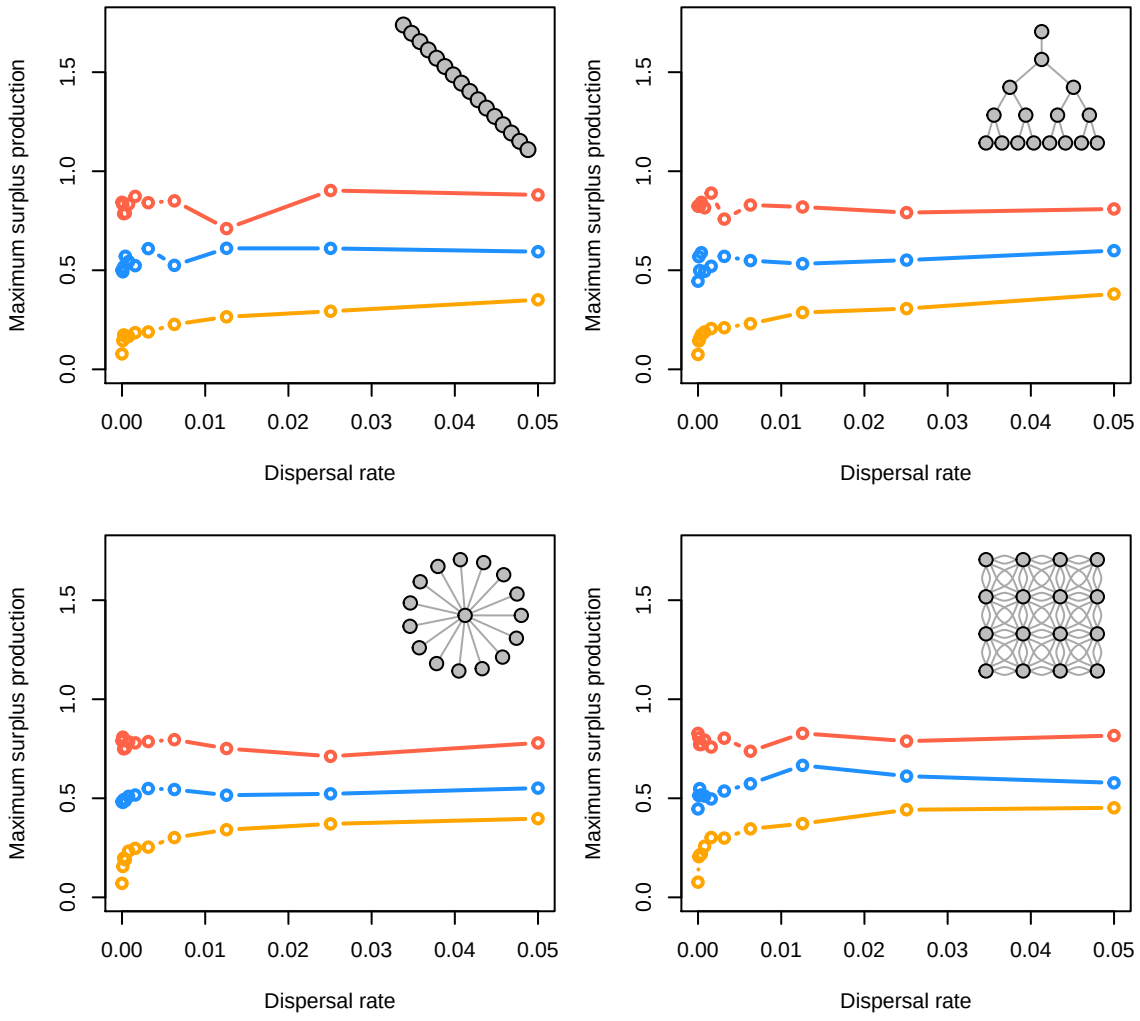

Figure S21: Maximum surplus production along dispersal, disturbance (red - uniform; blue - localized, random; orange - localized, extirpation), and network gradients with high spatial-temporal correlation in recruitment stochasticity and variable patches.

Patterns in the risk of hysteresis & state shifts

We now show similar patterns in the rate of long-term collapse across the metapopulation after 100 generations post-disturbance. Collapse rate % is defined as the number of simulations where metapopulation abundance failed to reach at least `1.0` of the average pre-disturbance abundance for `5` consecutive years after disturbance. This "collapse rate" reflects the risk of a long-term state shift in metapopulation dynamics after disturbance in the face of stochasticity. We start with a scenario with deterministic recruitment where patches are the same.

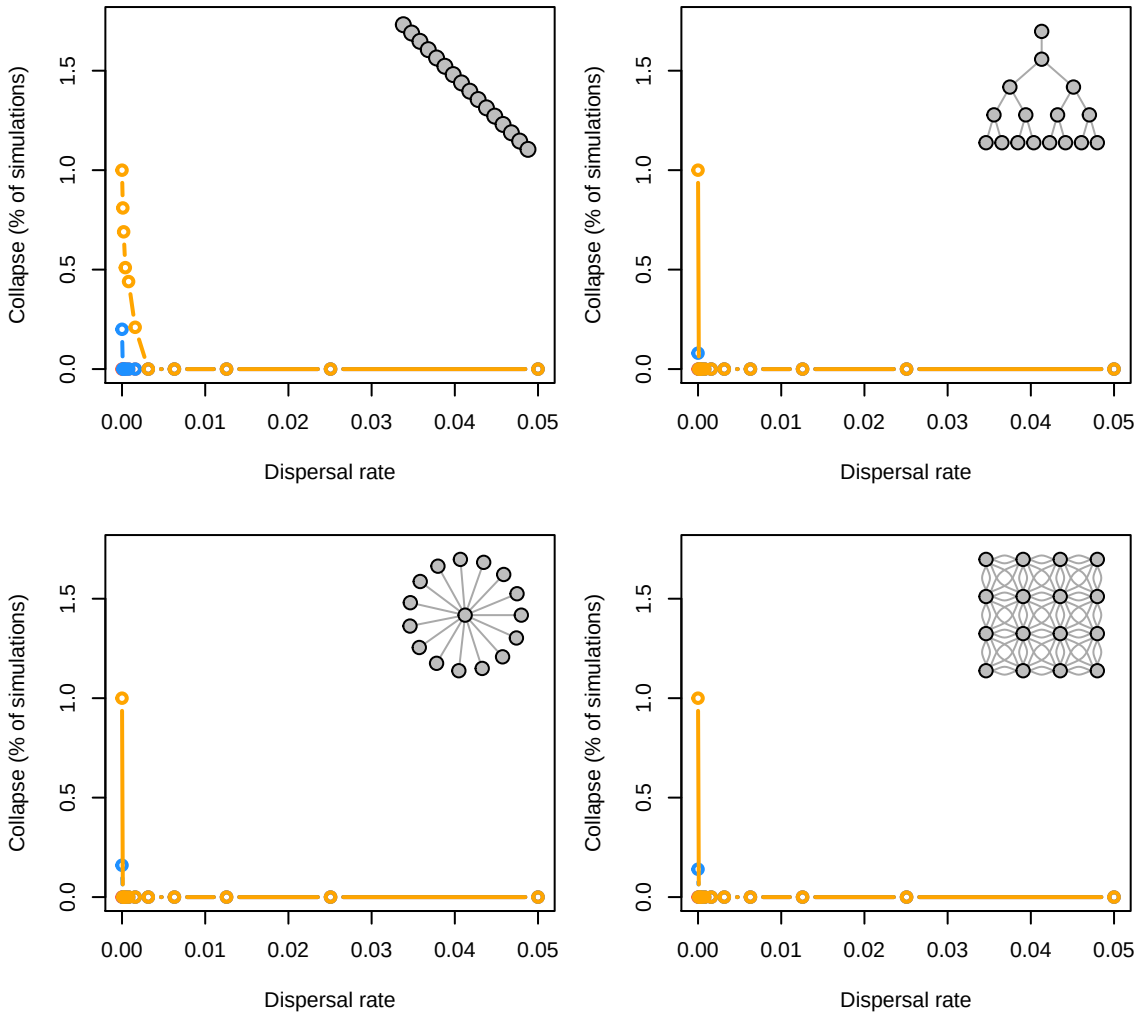

Figure S22: Risk of state shift after 100 generations along dispersal, disturbance (red - uniform; blue - localized, random; orange - localized, extirpation), and network gradients with high spatial-temporal correlation in recruitment variation.

291 **State shifts with variable patches**

292 Now, we illustrate how variable patch demography affects the risk of a state shift.

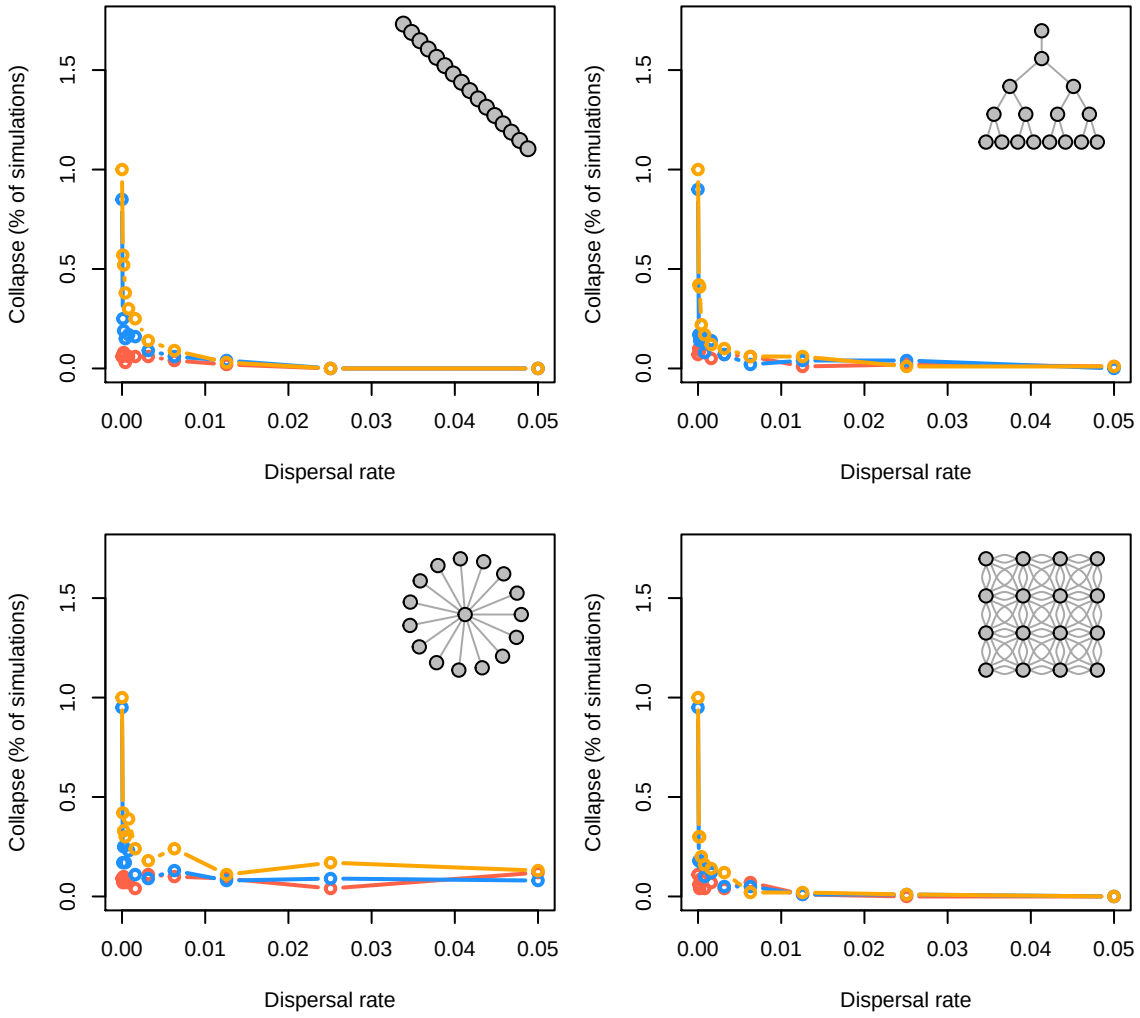

Figure S23: Risk of state shift after 100 generations along dispersal, disturbance (red - uniform; blue - localized, random; orange - localized, extirpation), and network gradients with variable patches.

293 **State shifts with variable patches and stochasticity**

294 Now, we illustrate how variable patch demography and stochastic recruitment affects the risk of state shift.

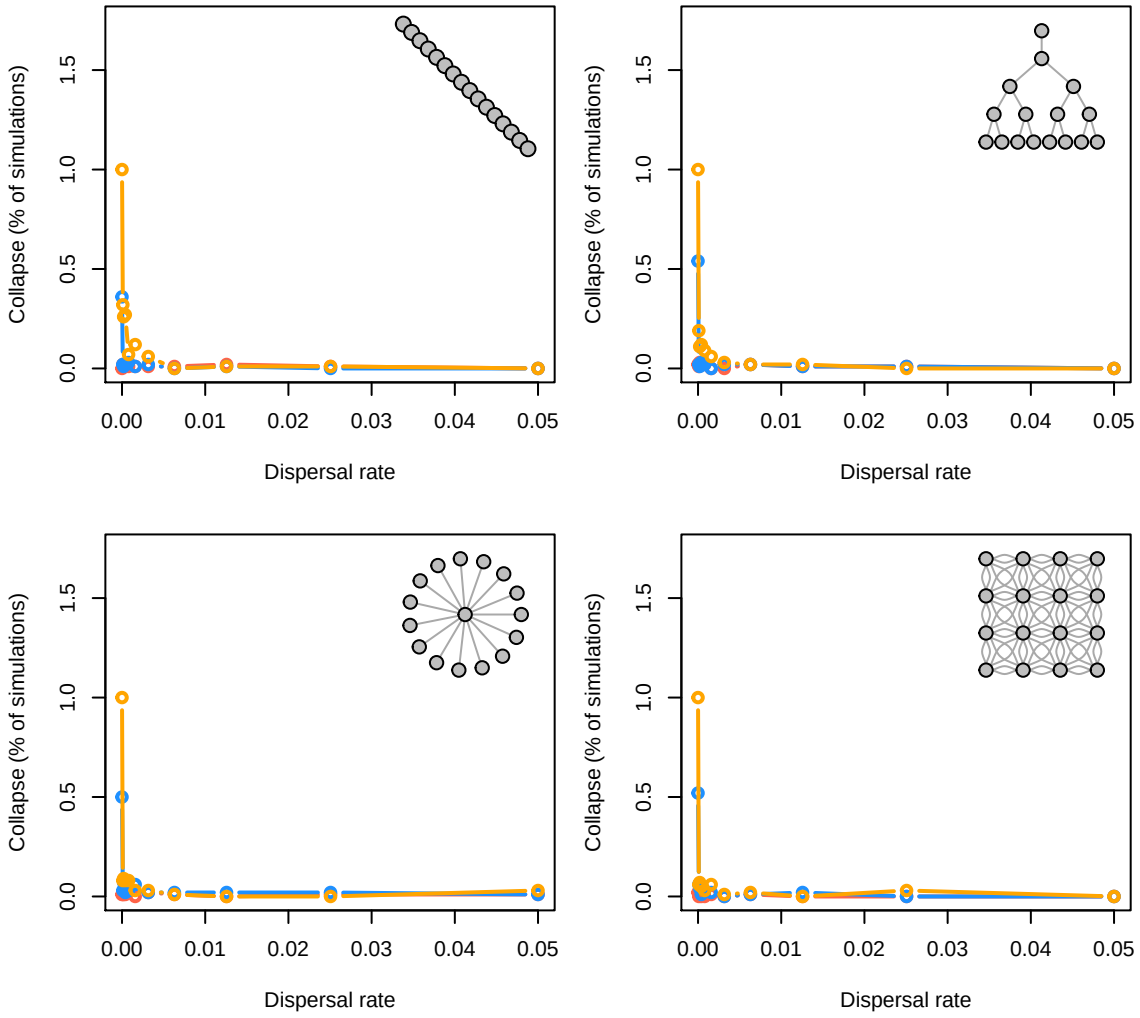

Figure S24: Risk of state shift after 100 generations along dispersal, disturbance (red - uniform; blue - localized, random; orange - localized, extirpation), and network gradients with variable patches and stochastic recruitment.

State shifts with variable patches, and spatio-temporally correlated stochasticity

Now, we illustrate how variable patch demography and high spatial-temporal correlations in stochastic recruitment affects the risk of a state shift.

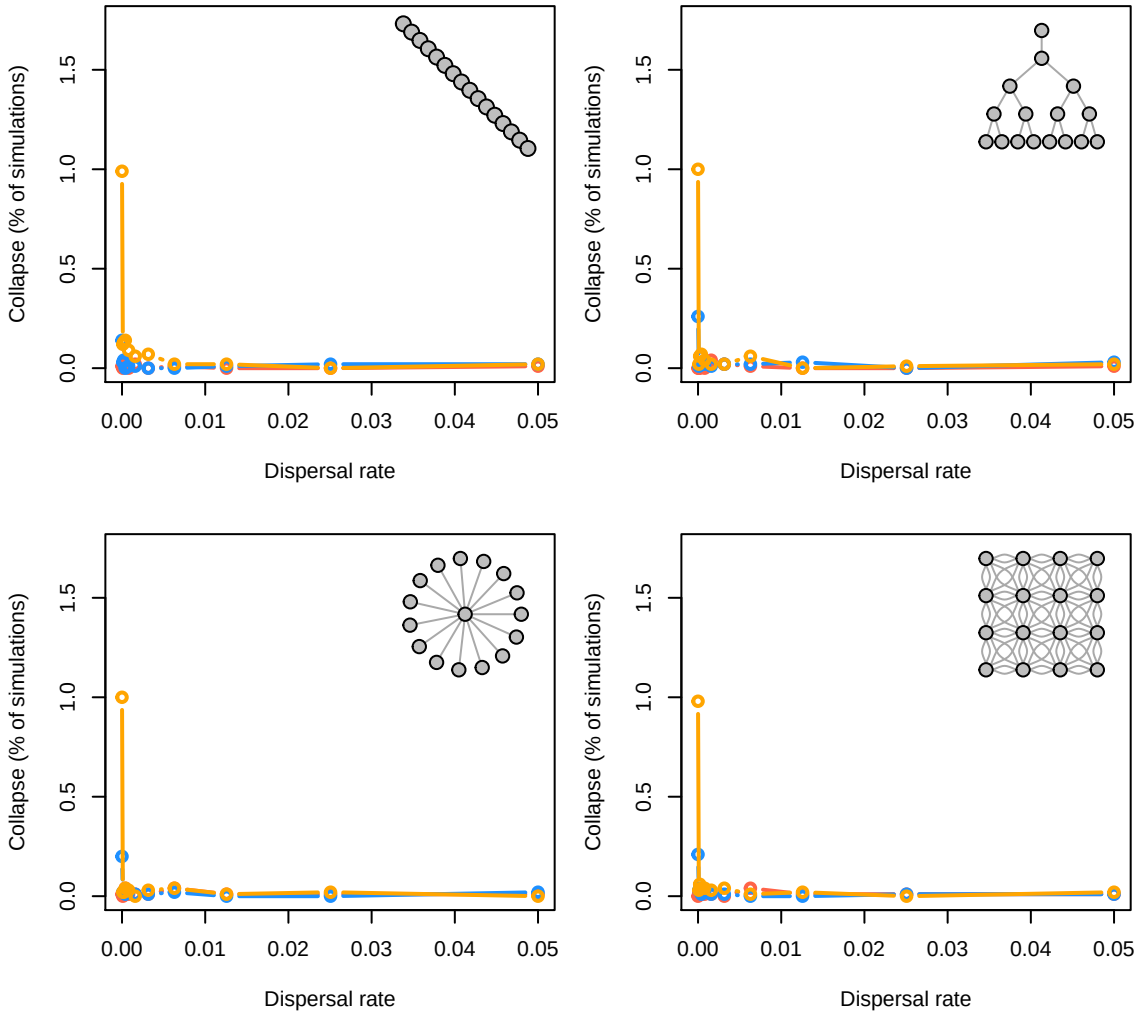

Figure S25: Risk of state shift (lack of recovery or spatial contraction) after 100 generations along dispersal, disturbance (red - uniform; blue - localized, random; orange - localized, extirpation), and network gradients with variable patches, and spatial-temporal correlations in stochastic recruitment.

Patterns in the risk of spatial contraction

We now show similar patterns in patch occupancy after 25 years post-disturbance. Patch occupancy is defined as the average number of patches that fail to recover above `0.1` pre-disturbance abundance for scenario with deterministic recruitment where patches are the same. Patch occupancy characterizes the expected risk of spatial contractions or local patch collapses, and reflects how interactions between spatial structure, disturbance, and dispersal affect source-sink dynamics and the provisioning of rescue effects to local patches.

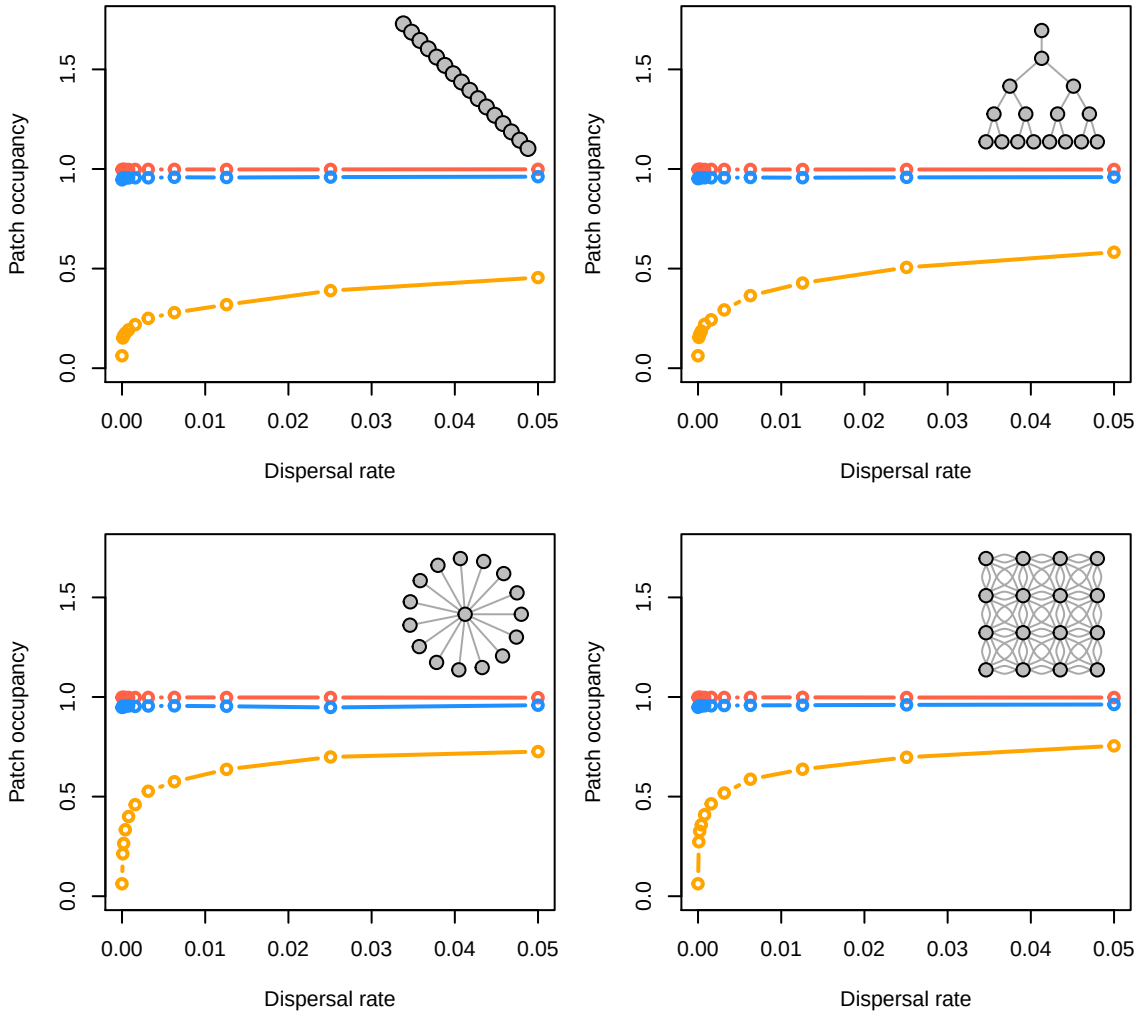

Figure S26: Patch occupancy after 25 years along dispersal, disturbance (red - uniform; blue - localized, random; orange - localized, extirpation), and network gradients with deterministic recruitment and homogeouns patches.

304 **Patch occupancy with variable patches**

305 Now, we illustrate how variable patch demography affects patch occupancy.

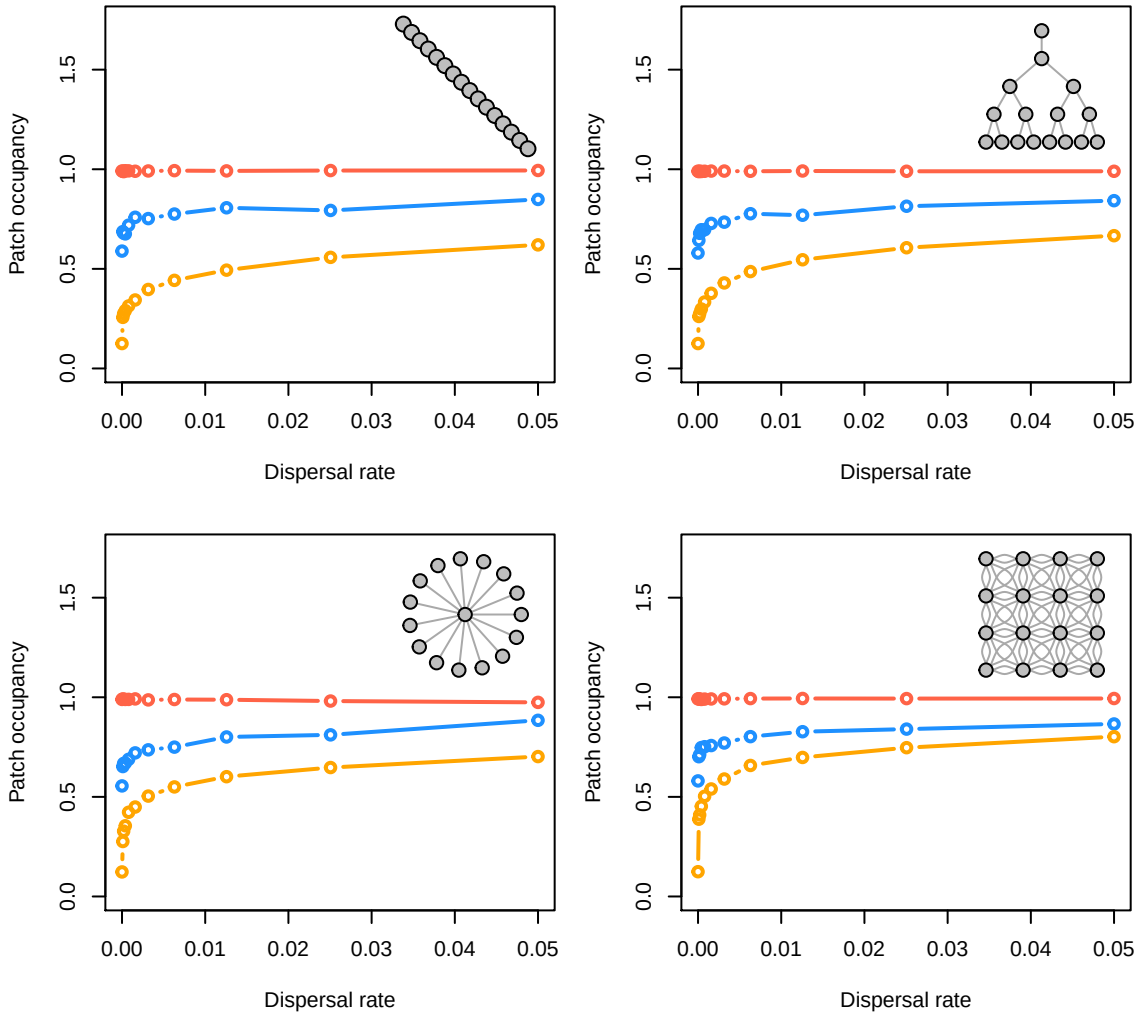

Figure S27: Patch occupancy after 25 years along dispersal, disturbance (red - uniform; blue - localized, random; orange - localized, extirpation), and network gradients with variable patches.

Patch occupancy with variable patches and stochasticity

Now, we illustrate how variable patch demography and stochastic recruitment affects long-term patch occupancy.

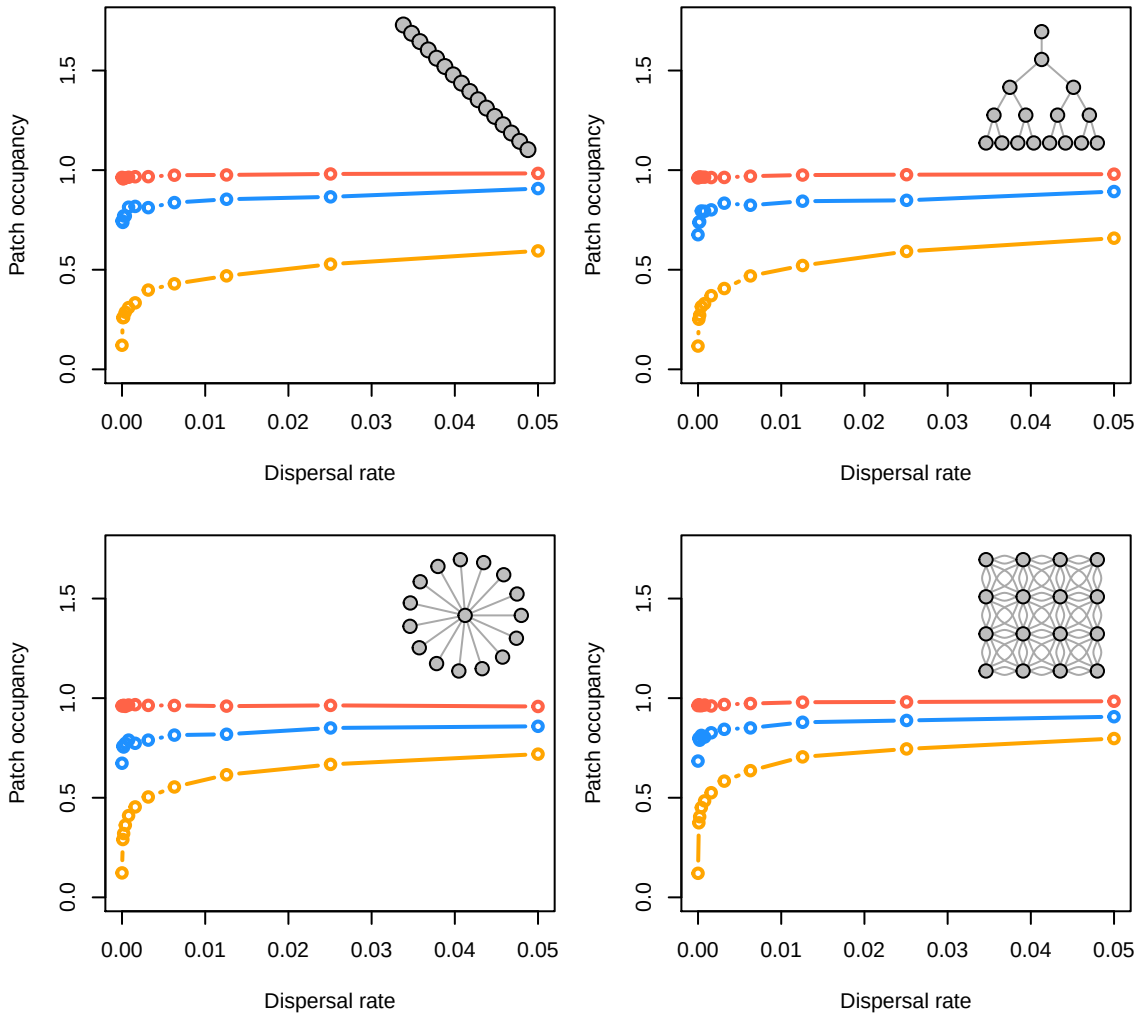

Figure S28: Patch occupancy after 25 years along dispersal, disturbance (red - uniform; blue - localized, random; orange - localized, extirpation), and network gradients with variable patches and stochastic recruitment.

Patch occupancy with variable patches and spatio-temporally correlated stochasticity in recruitment

Now, we illustrate how variable patch demography and high spatial-temporal correlations in stochastic recrtuitment affects long-term patch occupancy.

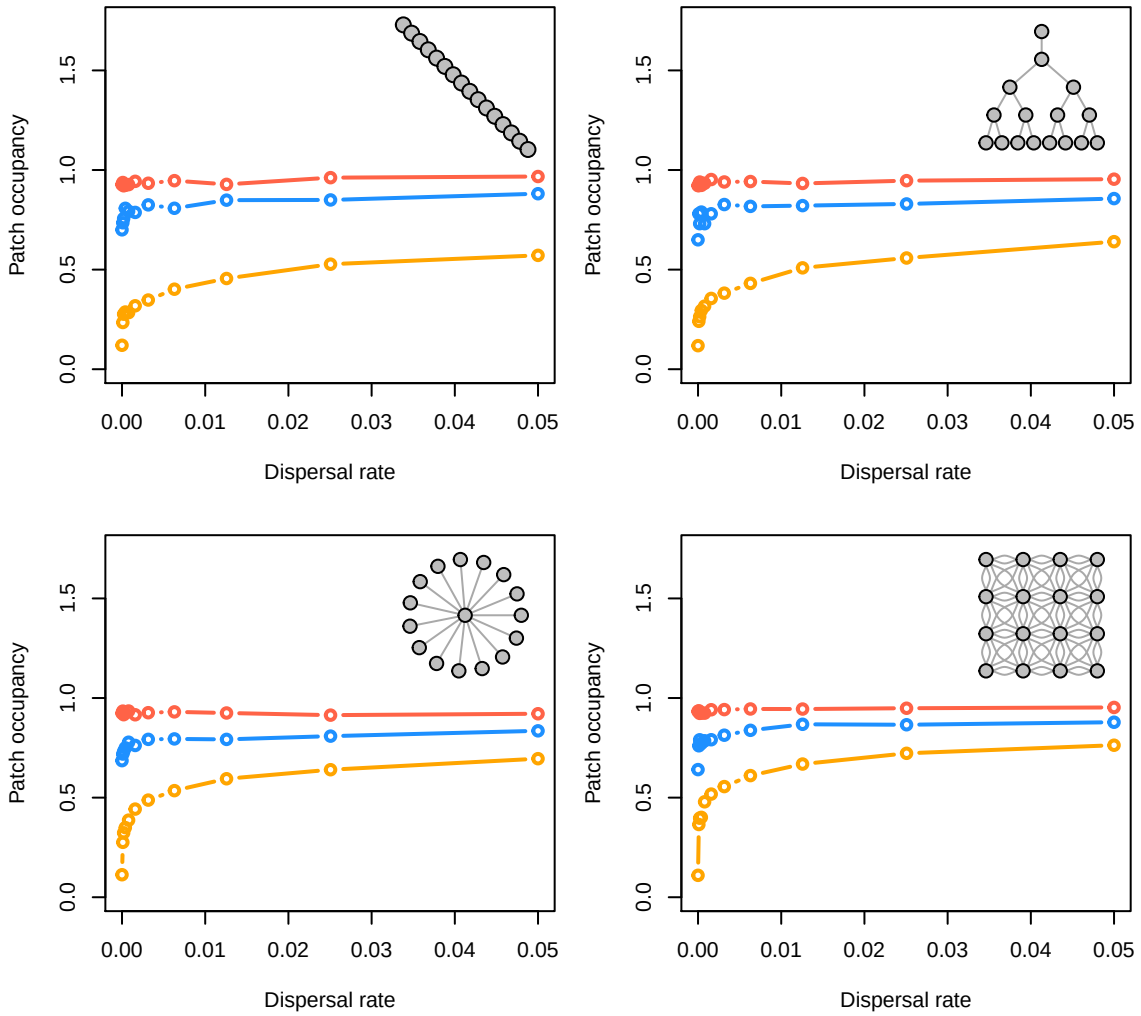

Figure S29: Patch occupancy after 25 years along dispersal, disturbance (red - uniform; blue - localized, random; orange - localized, extirpation), and network gradients with variable patches and spatial-temporal correlations in stochastic recruitment.

References

Anderson, S.C., Moore, J.W., McClure, M.M., Dulvy, N.K. & Cooper, A.B. (2015). Portfolio conservation of metapopulations under climate change. Ecological Applications 25 (2), 559-572. *Ecological Applications*, 25, 559–572.

Csardi, G. & Nepusz, T. (2006). The igraph software package for complex network research. *InterJournal*, Complex Systems, 1695.

Forrest, R.E., McAllister, M.K., Dorn, M.W., Martell, S.J. & Stanley, R.D. (2010). Hierarchical Bayesian estimation of recruitment parameters and reference points for Pacific rockfishes (Sebastes spp.) under alternative assumptions about the stock–recruit function. *Canadian Journal of Fisheries and Aquatic Sciences*, 67, 1611–1634.

Hanski, I. (1998). Metapopulation dynamics. *Nature*, 396, 41–49.

Yeakel, J.D., Moore, J.W., Guimarães, P.R. & Aguiar, M.A. de. (2014). Synchronisation and stability in river metapopulation networks. *Ecology Letters*, 17, 273–283.